




Article

Complex Analysis of the Efficiency of Difference Reflectance Indices on the Basis of 400–700 nm Wavelengths for Revealing the Influences of Water Shortage and Heating on Plant Seedlings

Ekaterina Sukhova ^{*} , Lyubov Yudina , Ekaterina Gromova, Anastasiia Ryabkova, Dmitry Kior and Vladimir Sukhov 

Department of Biophysics, N.I. Lobachevsky State University of Nizhny Novgorod, 603950 Nizhny Novgorod, Russia; lyubovsurova@mail.ru (L.Y.); kater333@inbox.ru (E.G.); nastay2903@bk.ru (A.R.); dimakior@mail.ru (D.K.); vssuh@mail.ru (V.S.)

* Correspondence: n.catherine@inbox.ru; Tel.: +7-929-040-2938

Abstract: A drought, which can be often accompanied by increased temperature, is a key adverse factor for agricultural plants. Remote sensing of early plant changes under water shortage is a prospective way to improve plant cultivation; in particular, the sensing can be based on measurement of difference reflectance indices (RIs). We complexly analyzed the efficiency of RIs based on 400–700 nm wavelengths for revealing the influences of water shortage and short-term heating on plant seedlings. We measured spectra of reflected light in leaves of pea, wheat, and pumpkin under control and stress conditions. All possible RIs in the 400–700 nm range were calculated, significances of differences between experimental and control indices were estimated, and heatmaps of the significances were constructed. It was shown that the water shortage (pea seedlings) changed absolute values of large quantity of calculated RIs. Absolute values of some RIs were significantly changed for 1–5 or 2–5 days of the water shortage; they were strongly correlated to the potential quantum yield of photosystem II and relative water content in leaves. In contrast, the short-term heating (pea, wheat, and pumpkin seedlings) mainly influenced light-induced changes in RIs. Our results show new RIs, which are potentially sensitive to the action of stressors.

Keywords: difference reflectance indices; stressor-induced changes; significance heatmaps; pea; wheat; pumpkin; water shortage; drought; heat; remote sensing



Citation: Sukhova, E.; Yudina, L.; Gromova, E.; Ryabkova, A.; Kior, D.; Sukhov, V. Complex Analysis of the Efficiency of Difference Reflectance Indices on the Basis of 400–700 nm Wavelengths for Revealing the Influences of Water Shortage and Heating on Plant Seedlings. *Remote Sens.* **2021**, *13*, 962. <https://doi.org/10.3390/rs13050962>

Academic Editor: Karel Charvat

Received: 29 January 2021

Accepted: 2 March 2021

Published: 4 March 2021

Publisher's Note: MDPI stays neutral with regard to jurisdictional claims in published maps and institutional affiliations.



Copyright: © 2021 by the authors. Licensee MDPI, Basel, Switzerland. This article is an open access article distributed under the terms and conditions of the Creative Commons Attribution (CC BY) license (<https://creativecommons.org/licenses/by/4.0/>).

1. Introduction

Plant cultivation is an important branch of the world's economy; the consumption of plant products increases from year to year. However, environmental conditions are rather variable [1–3]; the frequency and magnitude of fluctuations in these conditions can be stimulated under the development of global climate change. There are numerous stressors, including non-optimal temperatures, high intensities of light, excess precipitations, etc., which can decrease plant biomass and crop quality [4,5]. In particular, the factors strongly influence photosynthesis [6,7], which is a basis of plant productivity.

A soil drought is a key adverse factor for agricultural plants [5,8]. Water exchange and photosynthesis are important targets of the drought action [9,10]. Their changes are main reasons for the decrease in the plant productivity. The drought is often accompanied by the action of an increased temperature that can stimulate negative effects of the drought on the plant productivity [11]. It is important that even short-term water shortage (hours and days), which is induced by decreased irrigation [10,12] or the action of osmolitics [13,14], can induce numerous physiological and biochemical changes in plants. The short-term water shortage strongly influences photosynthetic processes and transpiration [10,12,14]; decreasing CO₂ assimilation and efficiency of photosynthetic machinery, inducing stomata

closing, suppressing water exchange, and increasing photosynthetic damage are the typical responses induced the shortage.

Thus, revealing the water shortage action early is a prospective method to minimize the photosynthetic damage and to protect crops. Developing methods of remote sensing of stress changes in plants (including drought- and heating-induced changes) [15–20] can be used for such revelation. These methods should be high-throughput, have spatial resolution, not influence plants and the environment [21], etc.

Optical methods (including multispectral, hyperspectral, fluorescence, thermal, and RGB imaging) are effective tools for plant monitoring (see, e.g., [15,21–24]). For example, measurements of solar-induced fluorescence can be used to estimate the rate of photosynthetic processes [24,25], including remote sensing of photosynthetic stress changes under the action of drought [26–28]. Thermal imaging can be used to estimate plant transpiration [29,30], including changes under the action of stressors; and RGB imaging can be used for remote sensing of plant growth and nitrogen nutrition status [31].

Measurements of spectra of reflected light can also be effectively used for estimation of plant physiological processes [18,21,22,32]. It is known that the spectra can be strongly related to photosynthetic processes [32–35], transpiration and water exchange [36–39], the content of pigments [18,40–46] and other biochemical compounds [47–49], ethylene emission [50,51], signaling processes [52–54], plant growth and development [22,55,56], etc. Changes in the spectra of reflected light can show responses of plants to short-term and long-term action of stressors [23,47,57–59].

However, interpreting the measured spectra of reflected light is an important problem of plant remote sensing. Developing methods of analysis of whole reflectance spectra (spectral “signatures” [60]) can be an effective solution of the problem. There are numerous works (e.g., [61–64]) that use methods of machine learning to analyze measurements of whole reflectance spectra and estimate the physiological processes in plants. However, machine learning has some limitations; in particular, deep learning, which may be the most prospective method in this group, requires large amounts of data for learning (e.g., thousands or tens of thousands of plant images with identified actions of stressors) [65,66]. Developing mechanistic models of radiative transfer in plant leaves and the canopy is an alternative method to analyze the relations between plant physiological processes and reflectance spectra. The models can be focused on the spectra of pigment absorption in the canopy (e.g., variants of PROSPECT [67–69]), the relationship of radiative transfer in leaves and canopy to photosynthetic processes [70–72], descriptions of topographic influences on plant reflectance [73], etc. Using these models can improve the reflectance analysis (e.g., to correct reflectance errors related to microslope topography [73] or to accurately estimate photosynthetic pigment content in plants [68,69]). The limitations of mechanistic models are mainly related to their complexity because descriptions of radiation transfer can be strongly dependent on the canopy geometry [72].

Another approach for the analysis of spectra of reflected light is to use narrowband [16–18] and broadband [22,53] reflectance indices (RIs), which show changes in reflected light intensity at a specific wavelength (measuring wavelength) relative to another wavelength (control wavelength). There are many widely used narrowband reflectance indices: normalized difference vegetation index (NDVI) [39,74,75], water index (WI) [36,76] and normalized difference water index (NDWI) [77], photochemical reflectance index (PRI) [33–35,42,48,78], near-infrared reflectance of terrestrial vegetation (NIR_V) [79], and others [18–22]. The application of reflectance indices has some advantages compared to other methods of analysis of plant reflectance spectra: (i) The possibility to measure based on both multi- and hyperspectral cameras; (ii) simple algorithms for calculating RIs; (iii) use of relative units for RIs and minimization of errors related to light intensity; and (iv) possibility to reveal specific physiological processes or specific physiological parameters related to specific wavelengths (e.g., WI and NDWI show water content in plants [36,54,76,77]; PRI is mainly caused by acidification in chloroplast lumen and shows photosynthetic processes [35,42,80]; etc.). The properties are the basis of using RIs in remote sensing of plant stress changes;

in particular, drought-induced plant changes can be revealed by measurements of NDVI and WI at different time and spatial scales [54,76,81–83]. Heating-induced changes in plants can also be revealed on the basis of the measurements of the indices [81,84].

However, further investigations into using RIs for estimating physiological processes in plants remain topical. Current RIs are calculated on the basis of analysis of only small amounts of potential combinations of spectral bands; at that, even small shifts of used wavelengths can modify sensitivities of the RIs to physiological processes (e.g., earlier we showed changes in relations between PRI and photosynthetic parameters under such shifts [59]). Solving this problem can be based on a complex analysis of the efficiency of all possible RIs, which are calculated based on all combinations of wavelengths of reflected light in a measured spectrum.

Only a few works have been devoted to this complex analysis [51,85–89]. Correlograms, which are heatmaps of the dependence of the correlation coefficient between RI and analyzed physiological parameters on the values of two wavelengths (used for RI calculation), are the main results of these investigations. Their use can simultaneously show relations of all possible reflectance indices with investigated physiological parameters [51,85,89]. Potentially, similar heatmaps of the significance (p) and directions of differences between spectral indices under control and experimental conditions can be used to quickly reveal RIs that are sensitive to actions of stressors including drought and heating; however, this possibility requires an experimental analysis.

The aim of our work was to conduct the complex analysis of the efficiency of using difference reflectance indices for early revealing the influences of the short-term water shortage and heating on plant seedlings. Our investigation was focused on the analysis of RIs calculated on the basis of 400–700 nm wavelengths which form a photosynthetic activity spectrum [90,91]. Considering the influence of the water shortage and heating on photosynthesis [7,10,12], the spectral range was expected to be sensitive to action of these stressors. The investigation was performed in laboratory conditions because investigations in controlled conditions are widely used approach for primary revealing effective RIs for remote sensing (see, e.g., [36] for WI, [77] for NDWI, and [33,48] for PRI).

2. Materials and Methods

2.1. Plant Materials and Treatments

We used two- to three-week-old seedlings of pea (*Pisum sativum* L., cultivar Albumen) for an investigation of short-term water shortage influence on RIs (in accordance with our previous work [92]). Plants were cultivated in a sand substrate in a Binder KBW 240 (Binder GmbH, Tuttlingen, Germany) under a 16/8 h (light/dark) photoperiod at 24 °C. The water shortage was emulated by irrigation absence for five days of the experiment. Control plants were irrigated every two days. Measurement of reflectance and photosynthetic parameters was performed every day of the water shortage for experimental and control seedlings. Quantities of investigated seedlings were 6 for plants under water shortage and 6 for control plants.

The relative water content in the sand substrate was measured as the ratio of difference between fresh and dry weights to fresh weight; the dry weight of sand was measured after 2 h of heating in a TV-20-PZ-K thermostat (Kasimov Instrument Plant, Kasimov, Russia) (about 100 °C). This content was rapidly decreased after the termination of irrigation: about 10% of water under control conditions, less than 5% of water on the first day of water shortage, and less than 0.5% on the following days of the shortage. The method was also used for estimation of the relative water content and dry weight in the leaves which were measured every day of water shortage in separate groups of seedlings. First, second, and third leaves from each investigated plant were analyzed; the relative water content and dry weight were calculated per leaf. Quantities of investigated seedlings were 6 for all experimental and control variants.

We used two- to three-week-old seedlings of pea (*Pisum sativum* L., cultivar Albumen), wheat (*Triticum aestivum* L., cultivar Zlata), and pumpkin (*Cucurbita pepo* L., cultivar

Mozoleevskaya) for the investigation of short-term heating influence on RIs (in accordance with [92]). The seedlings were hydroponically cultivated in the Binder KBW 240. The plants were heated in the thermostat for 30 min at 46.5 °C for pea and pumpkin and at 44 °C for wheat in accordance with our previous work [92]. Measurements of leaf plant reflectance and photosynthetic parameters for each seedling were performed on seedlings without heat (control plants) and in 1 h and one day after termination of heating (experimental plants). Quantities of control and heated seedlings were 5 for pea, 6 for wheat, and 6 for pumpkin.

2.2. Measurement of Reflected Light and Maximal Quantum Yield of Photosystem II

The measurement of the reflectance indices and photosynthetic parameters was performed on the second mature leaves of investigated plants (in accordance with our previous investigation [92]), which were kept at a fixed position (Figure 1).

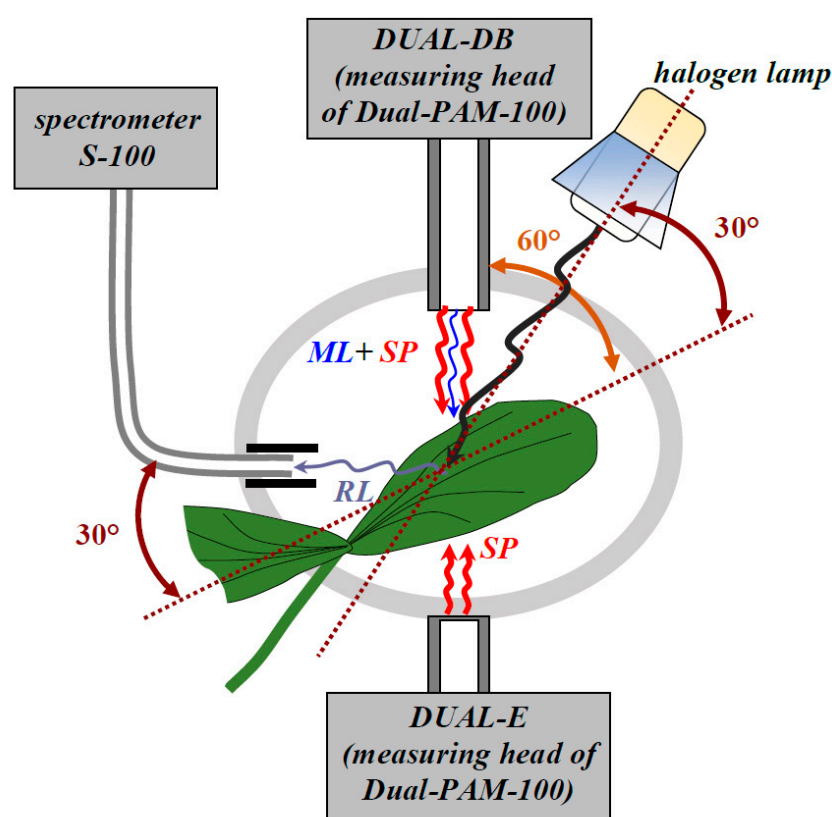


Figure 1. Schema of measurements of maximal quantum yield of photosystem II (F_v/F_m) and intensity of reflected light in leaves of pea, wheat, and pumpkin seedlings. Leaves of investigated plants were kept at a fixed angle. Measuring light (ML) refers to standard pulses of a weak blue light (460 nm, $24 \mu\text{mol m}^{-2} \text{s}^{-1}$, 2.5 μs pulse length). Saturation pulse (SP; red light, 630 nm, $10,000 \mu\text{mol m}^{-2} \text{s}^{-1}$, 300 ms) was used for estimation of F_v/F_m before illumination by white actinic light (AL). MLs and SPs were generated by Dual-PAM-100, including blocks DUAL-DB and DUAL-E. A halogen lamp Osram Decostar was used as a source of white AL (about $630 \mu\text{mol m}^{-2} \text{s}^{-1}$); duration of illumination was 9 min. Reflected light (RL) was measured by an S-100 spectrometer. Angle of light incidence on leaf surface was about 30°, angle between leaf surface and input for RL was about 30°, and angle between leaf surface and direction of SP and ML was about 60°.

The photosynthetic parameters and intensity of reflected light were simultaneously measured in leaves, as described in our previous works [52,80,92,93]. A halogen lamp (3000 K, 20 W, 12 V; Osram Decostar, OSRAM GmbH, Munich, Germany) was the source of white actinic light. The intensity of leaf illumination was about $630 \mu\text{mol m}^{-2} \text{s}^{-1}$. The distance from the halogen lamp to the leaf was about 15 cm; the angle between the

leaf's surface and the direction of the actinic light was about 30°. The white actinic light was turned on after the measurement of maximal quantum yield of photosystem II (Fv/Fm). The total duration of plant illumination by halogen lamp was about 9 min.

A Dual-PAM-100 PAM fluorometer (Heinz Walz GmbH, Effeltrich, Germany) was used to measure photosynthetic parameters. Plants were adapted under dark conditions for 15 min. The dark (Fo) and maximal (Fm) fluorescence yields in photosystem II (PSII) [24,94] were measured at the saturation pulse (630 nm, 10,000 $\mu\text{mol m}^{-2} \text{s}^{-1}$, 300 ms) before initiation of actinic light illumination and measurement of reflected light. In our investigation, we estimated the damage of the photosynthetic apparatus based on the value of Fv/Fm, which was calculated as:

$$\frac{F_v}{F_m} = \frac{F_m - F_o}{F_m}, \quad (1)$$

The intensity of reflected light by plant leaves was measured by using an S100 spectrometer (SOLAR Laser Systems, Minsk, Belarus) connected with a fiber optic cable. The tip of the cable was equipped with the simplest collimator as a small black tube. The geometry of the experiment is shown in Figure 1. The angle between the leaf's surface and the input of the fiber-optic cable was about 30°, and the distance from the leaf to the fiber-optic surface was about 1.5 cm. The spectral range of the S100 was 190–1050 nm, and the spectral resolution was about 1 nm. The white panel of a QPcard 101 calibration card ver. 3 (Argraph Corp., Carlstadt, NJ, USA) was used for the calibration procedure before measuring the spectra of reflected light in leaves.

The integration time was 5 s, and continuously repeating measurements were used. We used two time points for our analysis: after turning on the halogen lamp and after 7 min of illumination. The final intensity of reflected light at both time points was calculated as the difference between this intensity under illumination and the dark rate of the signal.

2.3. Calculation of Difference Reflectance Indices and Data Analysis

The calculation of difference reflectance indices and data analysis were based on several programs, which were developed using the Python 3.8 programming language. These programs solved the following tasks:

- (i) Calculation of all possible difference RIs according to Equation (2):

$$RI = \frac{I(R_1) - I(R_2)}{I(R_1) + I(R_2)}, \quad (2)$$

where $I(R_1)$ and $I(R_2)$ are intensities of reflected light at R_1 and R_2 wavelengths (in the spectral range from 400 to 700 nm). The intensities were averaged in a 3 nm range for increasing accuracy of the analysis. If $R_2 \geq R_1$ then RI was not calculated. Additionally, light-induced changes in RIs (ΔRIs) were calculated according to Equation (3):

$$\Delta RI = RI_2 - RI_1, \quad (3)$$

where RI_1 was calculated based on $I(R_1)$ and $I(R_2)$, which were measured immediately after turning on the halogen lamp (first time point), and RI_2 was calculated based on $I(R_1)$ and $I(R_2)$, which were measured 7 min after turning on the halogen lamp (second time point).

- (ii) Calculation of significance (p) of differences between control and experimental plants for all calculated RIs (or ΔRIs); the nonparametric Mann–Whitney U test was used for estimation of p . Directions of changes were also estimated. Two-dimensional data arrays (significances and directions of changes for each RI as function of R_1 and R_2) were results of this stage of the analysis. The arrays were used for direct revealing the effective RIs (or ΔRIs) or for following construction of heatmaps.
- (iii) Construction of two-dimensional heatmaps based on the arrays. Each pixel of the heatmaps could show three variants (different colors): significant increase of the experimental RI or ΔRI ($p \leq 0.05$, increase), significant decrease of the experimental

RI or Δ RI ($p \leq 0.05$, decrease), and absence of significant difference between control and experimental RI or Δ RI ($p > 0.05$).

NDVI (Equation (4)) and WI (Equation (5)) were additionally calculated in the experiments because the indices could be used for estimating drought and heating action [54,76,81–84]:

$$\text{NDVI} = \frac{I(764 - 796) - I(664 - 676)}{I(764 - 796) + I(664 - 676)}, \quad (4)$$

where $I(764-796)$ and $I(664-676)$ are the intensities of reflected light averaged in 764–796 nm and 664–676 nm ranges, respectively [75].

$$\text{WI} = \frac{I(900)}{I(970)}, \quad (5)$$

where $I(900)$ and $I(970)$ were intensities of reflected light at 900 and 970 nm, respectively [76].

2.4. Statistics

Considering the quantity of repetitions equaling 5–6, their distributions could be differed from the normal distribution. As a result, we preliminarily used the Shapiro–Wilk test for estimation of normality of distributions of calculated RIs, Δ RI, NDVI, WI, F_v/F_m , and relative water content in control and experiments. The most of investigated parameters had the normal distribution (data not shown); however, there were parameters which had not the normal distribution and could not analyzed by methods of parametric statistical analysis (e.g., Student's t-test). For standardization of the analysis, we used the nonparametric Mann–Whitney U test calculated by using the Python 3.8 for analysis of all investigated parameters. Medians of investigated values were used as a nonparametric analog of averaged values.

In experiments with water shortage, linear correlation coefficients between calculated reflectance indices and investigated physiological parameters (F_v/F_m , relative water content) were calculated. Medians, which were separately calculated on the basis of control and experimental values for each day of the water shortage, were used for the calculation ($n = 10$).

3. Results

3.1. Influence of Water Shortage on Relative Water Content and Maximal Quantum Yield of Photosystem II

On the first stage of the investigation, we analyzed influencing water shortage on the relative water content, F_v/F_m , and dry weight of leaves of pea seedlings. The water shortage was emulated by the absence of irrigation for five days; this water regime quickly decreased the water content in the sand substrate. Only pea seedlings were used in this experimental variant because our preliminary experiments showed that they were sensitive to the water shortage and suitable for investigation of the influence of water deficit on photosynthetic and spectral properties of leaves [54,92].

Figure 2a shows that the water shortage decreased the relative water content in leaves. The significant decrease was initiated in the second day of water shortage and was about 17% in the fifth day. The result showed that decrease of the soil relative water content induced decrease of the leaf relative water content for the investigated time interval. Figure 2b shows that significant decrease of F_v/F_m was observed for 2–5 days of the water shortage development. The strong decrease of F_v/F_m , which probably indicated damage of photosynthetic machinery, was observed on the fourth day, and especially the fifth day of the water shortage action. In contrast, Figure 2c shows that the dry weight was not significantly changed for five days under the irrigation absence.

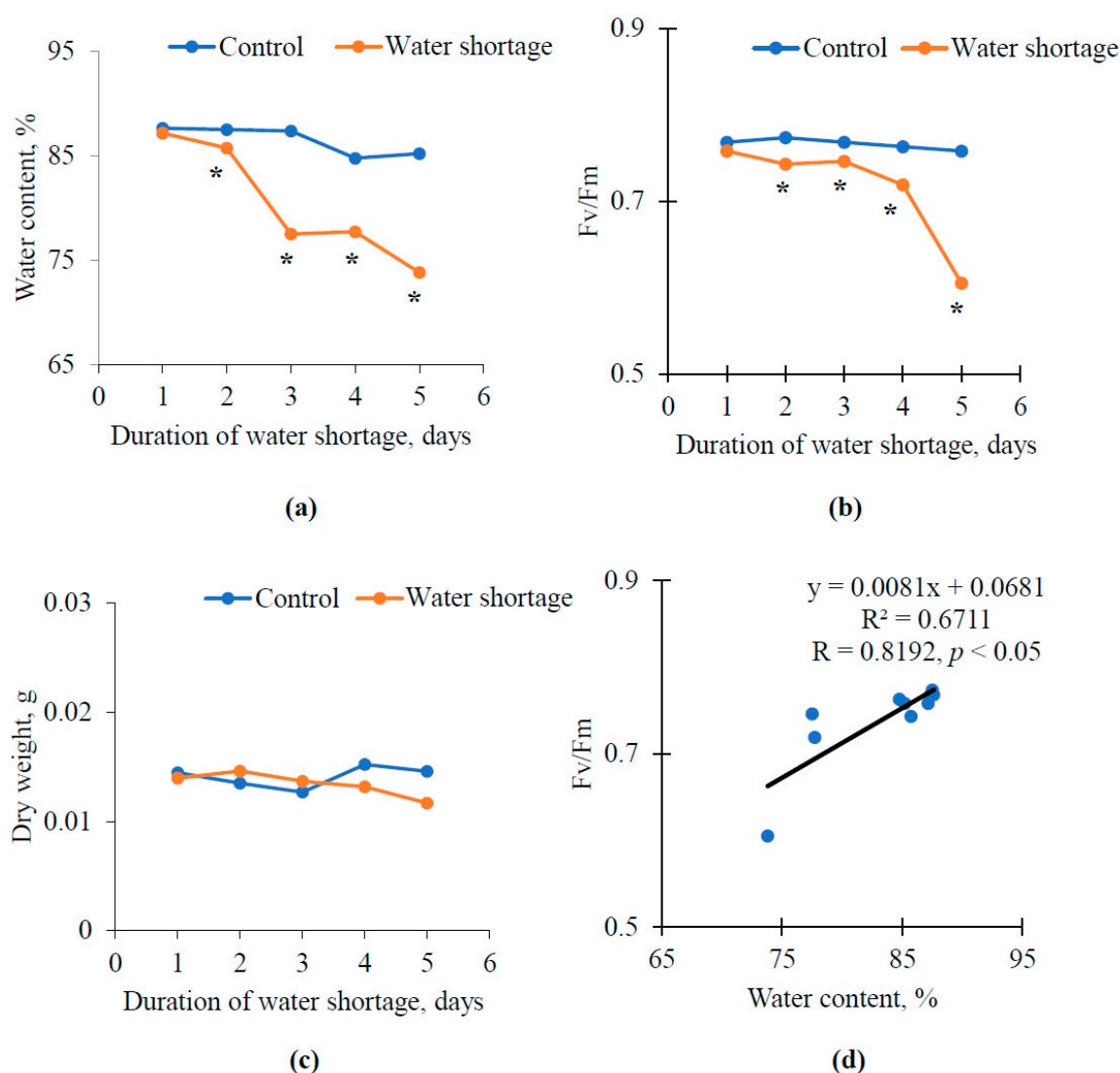


Figure 2. Dynamics of the relative water content (a), photosynthetic maximal quantum yield (Fv/Fm) (b), and dry weight (c) in leaves of pea seedlings subjected to the water shortage and a scatter plot between the relative water content and Fv/Fm (d). The relative water content and dry weight were calculated per leaf. Control plants were irrigated every two days, irrigation was not used for five days in experiment. R^2 and R are determination and correlation coefficients. Medians are shown in the figure. * Value significantly differed from control ($p < 0.05$, Mann–Whitney U test).

After that, we investigated relations between the decrease of the leaf relative water content and the Fv/Fm decrease. Medians, which were separately calculated for values in control and experimental seedlings in each day of the water shortage, were used for calculation of correlation coefficient. Figure 2d shows that the relative water content in leaves and Fv/Fm were strongly related at the water shortage (R was about 0.82). The result showed that the water loss was probable to induce the photosynthetic damage at the emulated water shortage. Thus, this experimental variant could be used for further investigation of the influence of the water shortage on the RIs of pea leaves.

3.2. Influence of Water Shortage on Difference Reflectance Indices

Further, we investigated influencing the water shortage on difference reflectance indices in leaves of pea seedlings (Figures 3 and 4). Heatmaps for significances and directions of water shortage-induced changes in RIs and Δ RIs, which were calculated on the basis of wavelengths in the 400–700 nm range, were constructed for each day of the water shortage action.

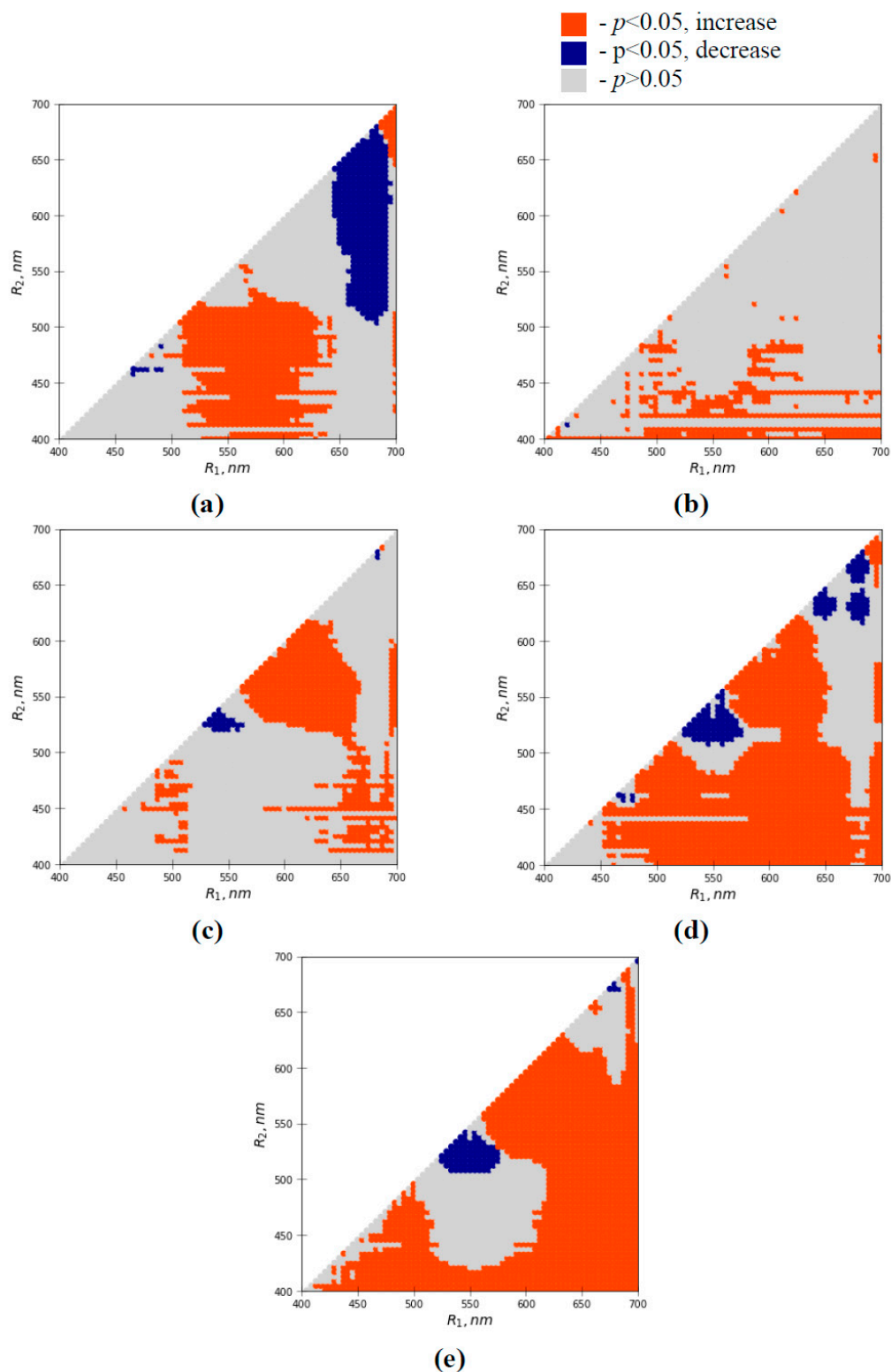


Figure 3. Heatmaps of significances and directions of water shortage-induced changes in absolute values of RIs in pea leaves in the first (a), second (b), third (c), fourth (d), and fifth (e) days of the water shortage. RIs were calculated based on equation $RI = \frac{I(R_1) - I(R_2)}{I(R_1) + I(R_2)}$, where $I(R_1)$ and $I(R_2)$ are intensities of reflected light at different narrow spectral bands (averaged for 3 nm). The Mann–Whitney U test was used for p calculations.

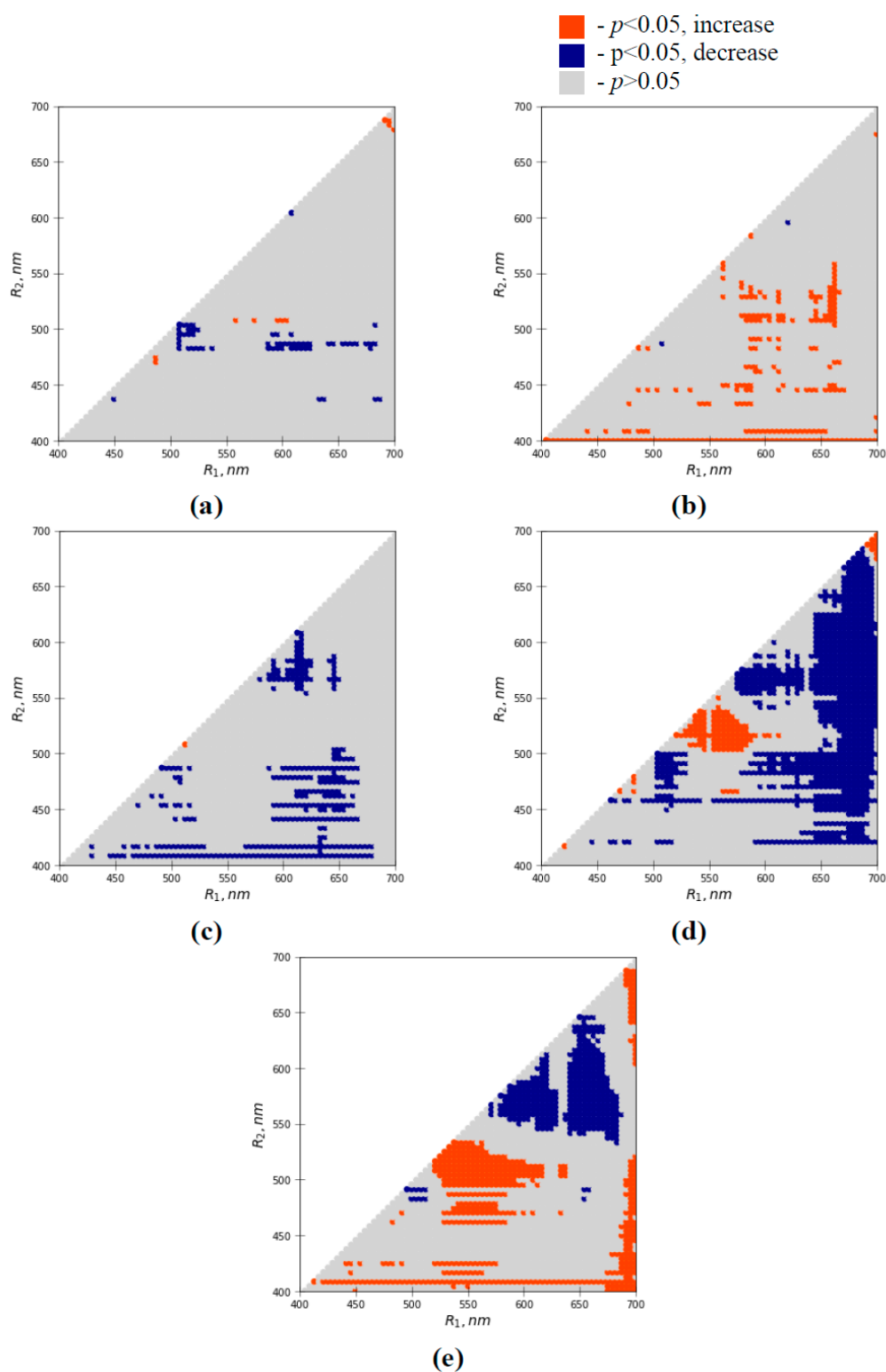


Figure 4. Heatmaps of significances and directions of water shortage-induced changes in Δ RIs in pea leaves in the first (a), second (b), third (c), fourth (d), and fifth (e) days of the water shortage. RIs were calculated based on equation $RI = \frac{I(R_1) - I(R_2)}{I(R_1) + I(R_2)}$, where $I(R_1)$ and $I(R_2)$ are intensities of reflected light at different narrow spectral bands (averaged for 3 nm). Δ RI (the light-induced change in RI) was calculated as $RI_2 - RI_1$. RI_1 was calculated based on $I(R_1)$ and $I(R_2)$ measured immediately after turning on the halogen lamp (first time point), and RI_2 based on $I(R_1)$ and $I(R_2)$ measured 7 min after turning on lamp (second time point). The Mann–Whitney U test was used for p calculations.

Figure 3 shows heatmaps of significances and directions of water shortage-induced changes in absolute values of RIs in pea leaves in different days of the water shortage. Two large spectral regions with significant differences between control and experimental seedlings (with increased and with decreased RIs) and several small regions were observed in the first day of the water shortage. In the second day, regions with decreased RIs were absent (excluding separate pixels or small groups of pixels) and areas of spectral regions with increased RIs were strongly reduced. Since the third day of the water shortage, areas of spectral regions with significant changes in RIs were increased. On the fifth day of the water shortage, areas of the spectral regions with significant changes in absolute values of RIs formed the most part of total area of the heatmap (about 71%).

Figure 4 shows heatmaps of significances and directions of water shortage-induced changes in Δ RIs (the light-induced change in RIs) in pea leaves in different days of the water shortage. There were only small spectral regions and separate pixels in the heatmaps with significant differences between control Δ RIs in experimental and control plants in the first, second, and third days of the water shortage. Positions of the regions and pixels were varied in different days of the water shortage. Since the fourth day of the water shortage, large spectral regions with positive and negative changes in Δ RIs were observed. In the fifth day of the water shortage, areas of the spectral regions with significant changes in Δ RIs were about 30% from total area of the heatmap.

The results showed that the water shortage action could influence the number of RIs; changes in their absolute values were more expressive than changes in Δ RIs. Several spectral regions with significant differences between RIs (or Δ RIs) were observed in specific days of the water shortage. For example, a large spectral region with decreased RIs (R_1 was about 640–690 nm, R_2 was about 500–650 nm) was revealed in the first day (Figure 3a) but it was absent in the second day (Figure 3b). In contrast, there were spectral regions with significant differences which were observed for several days of the water shortage. For example, a large spectral region with increased RIs (R_1 was about 560–640 nm, R_2 was about 520–600 nm) was observed since the third day of the water shortage (Figure 3c–e).

3.3. Analysis of Efficiencies of Difference Reflectance Indices for Revealing Water Shortage-Induced Changes in Seedlings

In the next stage of our work, we directly analyzed the two-dimensional data arrays, which included significances and directions of changes for each RI as function of R_1 and R_2 . Revealing RIs, which were changed on initial stages of the water shortage and remained changed after that, was main task of this analysis because the indices could be potentially considered as markers of action of drought on plants.

Table 1 shows that there were only a small portion of RIs (less than 2%), which were significantly changed for 1–5 or 2–5 days of the water shortage. In contrast, about 25% of the total quantity of RIs was changed for 3–5 days of the water shortage and more than 50% of all RIs was changed for 4–5 days of the water shortage. Percentages of changed Δ RIs were lower, e.g., about 15% was changed for 4–5 days of the soil water shortage.

Table 1. Percentages of RIs and Δ RIs, which were significantly changed for different time intervals after the water shortage initiation.

Title 1	1–5 Days	2–5 Days	3–5 Days	4–5 Days	5 Days
RIs	0.1903%	1.7504%	22.8691%	51.0274%	71.1568%
Δ RIs	0%	0%	1.5221%	15.6012%	31.3166%

RIs, which were significant changed for 1–5 and 2–5 days of the water shortage, were the most interesting for analysis because they were sensitive to the earliest action of the water shortage. Table 2 shows these RIs and their correlations with the relative water content and Fv/Fm in leaves of pea seedlings. Only absolute values of RIs were analyzed. Additionally, Table 2 shows NDVI and WI, which are widely used indices for estimating the drought action on plants [54,76,81–83].

Table 2. Time ranges of efficiencies of absolute values of RIs for the water shortage sensing and correlation coefficients between RIs and investigated physiological parameters (Fv/Fm and the relative water content in leaves). Correlation coefficients with absolute values more than 0.90 are marked by bold.

Index	R ₁ , nm	R ₂ , nm	Time Range of RI Efficiency ($p < 0.05$)	Correlation Coefficient between RI and Fv/Fm	Correlation Coefficient between RI and Water Content	Direction of Changes in RI
NDVI	764–796 (780)	664–677 (670)	3–5 days	0.9513 *	0.8931 *	decrease
WI	900	970	5 day	0.4052	0.6318	decrease
RI 1	621	442	1–5 days	−0.7435 *	−0.8618 *	increase
RI 2	629	442	1–5 days	−0.7606 *	−0.8814 *	increase
RI 3	633	442	1–5 days	−0.7539 *	−0.8576 *	increase
RI 4	637	442	1–5 days	−0.7636 *	−0.8654 *	increase
RI 5	700	442	1–5 days	−0.7223 *	−0.8281 *	increase
RI 6	475	450	2–5 days	−0.6312	−0.8849 *	increase
RI 7	487	421	2–5 days	−0.8396 *	−0.8985 *	increase
RI 8	487	458	2–5 days	−0.7208 *	−0.8039 *	increase
RI 9	491	421	2–5 days	−0.8666 *	−0.8983 *	increase
RI 10	496	421	2–5 days	−0.8326 *	−0.9099 *	increase
RI 11	496	479	2–5 days	−0.6760 *	−0.8831 *	increase
RI 12	496	483	2–5 days	−0.6754 *	−0.8997 *	increase
RI 13	500	421	2–5 days	−0.8300 *	−0.9272 *	increase
RI 14	500	450	2–5 days	−0.7071 *	−0.9244 *	increase
RI 15	500	471	2–5 days	−0.8178 *	−0.9721 *	increase
RI 16	500	479	2–5 days	−0.6811 *	−0.9096 *	increase
RI 17	500	483	2–5 days	−0.7159 *	−0.9491 *	increase
RI 18	504	421	2–5 days	−0.8219 *	−0.9346 *	increase
RI 19	504	450	2–5 days	−0.7061 *	−0.9328 *	increase
RI 20	504	471	2–5 days	−0.7963 *	−0.9404 *	increase
RI 21	504	479	2–5 days	−0.7075 *	−0.9309 *	increase
RI 22	508	421	2–5 days	−0.7957 *	−0.9308 *	increase
RI 23	512	421	2–5 days	−0.7642 *	−0.9077 *	increase
RI 24	613	604	2–5 days	−0.9252 *	−0.9184 *	increase
RI 25	629	421	2–5 days	−0.7970 *	−0.8835 *	increase
RI 26	633	421	2–5 days	−0.7998 *	−0.8851 *	increase
RI 27	637	421	2–5 days	−0.7968 *	−0.8817 *	increase
RI 28	654	421	2–5 days	−0.8061 *	−0.9084 *	increase
RI 29	654	442	2–5 days	−0.8077 *	−0.9210 *	increase
RI 30	658	421	2–5 days	−0.8101 *	−0.9074 *	increase
RI 31	658	442	2–5 days	−0.8099 *	−0.9202 *	increase
RI 32	662	421	2–5 days	−0.8173 *	−0.9121 *	increase
RI 33	662	442	2–5 days	−0.8173 *	−0.9213 *	increase
RI 34	667	421	2–5 days	−0.8183 *	−0.9063 *	increase
RI 35	667	442	2–5 days	−0.8166 *	−0.9135 *	increase
RI 36	671	421	2–5 days	−0.8153 *	−0.9033 *	increase
RI 37	671	433	2–5 days	−0.8441 *	−0.8884 *	increase
RI 38	675	421	2–5 days	−0.8237 *	−0.9037 *	increase
RI 39	679	421	2–5 days	−0.8288 *	−0.9027 *	increase
RI 40	683	421	2–5 days	−0.8317 *	−0.8973 *	increase
RI 41	687	421	2–5 days	−0.8399 *	−0.9041 *	increase
RI 42	687	433	2–5 days	−0.8822 *	−0.8702 *	increase
RI 43	692	421	2–5 days	−0.8431 *	−0.9067 *	increase
RI 44	692	442	2–5 days	−0.8250 *	−0.9145 *	increase
RI 45	696	421	2–5 days	−0.8414 *	−0.9190 *	increase
RI 46	696	442	2–5 days	−0.8020 *	−0.9117 *	increase

*, the correlation coefficient was significant. Correlation coefficients were calculated on the basis of medians of values of RIs in control and experimental seedlings; the averaging was performed for each day of the water shortage ($n = 10$).

Table 2 shows that there were five reflectance indices, which were significantly increased since the first day of the water shortage, and another 41 reflectance indices, which were significantly increased since the second day of the water shortage. The most of these RIs were strongly correlated with F_v/F_m and the relative water content in leaves of pea seedlings. NDVI was also strongly related to the physiological parameters; however, it was significantly changed since the third day of the water shortage. Correlation coefficients between WI and investigated physiological parameters were lower than ones for other RIs (e.g., the coefficient between WI and the relative water content was 0.63). The result was in a good accordance with literature data [76] which showed that average correlation coefficient between WI and the relative water content was about 0.66. Significant change in WI was observed in the fifth day of the water shortage. Thus, revealed RIs seemed to be more effective markers of the water shortage action in investigated plants than NDVI and WI.

Dynamics of NDVI, WI, and several revealed RIs in control and experimental pea seedlings were separately investigated. We analyzed the $RI(621,442)$ calculated on the basis of reflected light intensities at 621 and 442 nm, $RI(500,471)$ calculated on the basis of reflected light intensities at 500 and 471 nm, and $RI(692,421)$ calculated on the basis of reflected light intensities at 692 and 421 nm. $RI(621,442)$ was selected because it was significantly changed for 1–5 days of the water shortage. $RI(500,471)$ and $RI(692,421)$ were selected because they were calculated on the basis of different spectral regions (green-blue and red-blue regions, respectively) and were strongly correlated to physiological parameters.

Figure 5 shows that all selected RIs had relatively stable dynamics in control plants; in contrast, the NDVI and, especially, WI dynamics were more varied under control conditions. A magnitude of $RI(692,421)$ changes was more than the magnitude of NDVI changes (about 0.2 and about 0.3, respectively). The magnitudes of $RI(621,442)$ and $RI(500,471)$ changes were lower (about 0.015 and about 0.05, respectively); however, the magnitudes were comparable to the magnitudes of other widely-used reflectance indices (e.g., PRI [59]).

3.4. Influence of Short-Term Heating on Maximal Quantum Yield of Photosystem II and Difference Reflectance Indices

It is known [11] that development of soil drought is often accompanied by increased temperature actions; at that, durations of these actions (daily temperature changes and/or direct heating of leaves induced by sunlight) can be strongly shorter than the duration of soil drought. Considering this point, we additionally investigated influencing the short-term heating on F_v/F_m and reflectance indices. Earlier, we showed that the short-term heating could strongly influence photosynthetic parameters and PRI in pea, wheat, and pumpkin seedlings [92]. As a result, wheat and pumpkin seedlings were additionally investigated in the experiment with the short-term heating. Experimental F_v/F_m and reflectance indices were measured in 1 h and one day after the action of high temperature on seedlings of pea, wheat, and pumpkin.

It was shown that F_v/F_m was significantly decreased in 1 h after the short-term heating in pea, wheat, and pumpkin seedlings (Figure 6). In pea, F_v/F_m did not recover in one day after the heating. In wheat and pumpkin, F_v/F_m partially recovered in this time.

Figure 7 shows that heatmaps of significances and directions of heating-induced changes in absolute values of RIs. Two large spectral regions with significant differences between control and experimental seedlings (with increased and decreased RIs) and several small regions were observed in pea and pumpkin leaves in 1 h after the heating. The spectral regions with increased RIs were strongly decreased in one day after the heating (especially, in pumpkin leaves); the spectral regions with decreased RIs were practically absent after this time interval. In wheat seedlings, there were only several small spectral regions (and separate pixels) with significantly increased absolute values of RIs in 1 h and one day after the short-term heating. Spectral regions and separate pixels with decreased absolute values of RIs were absent in wheat seedling.

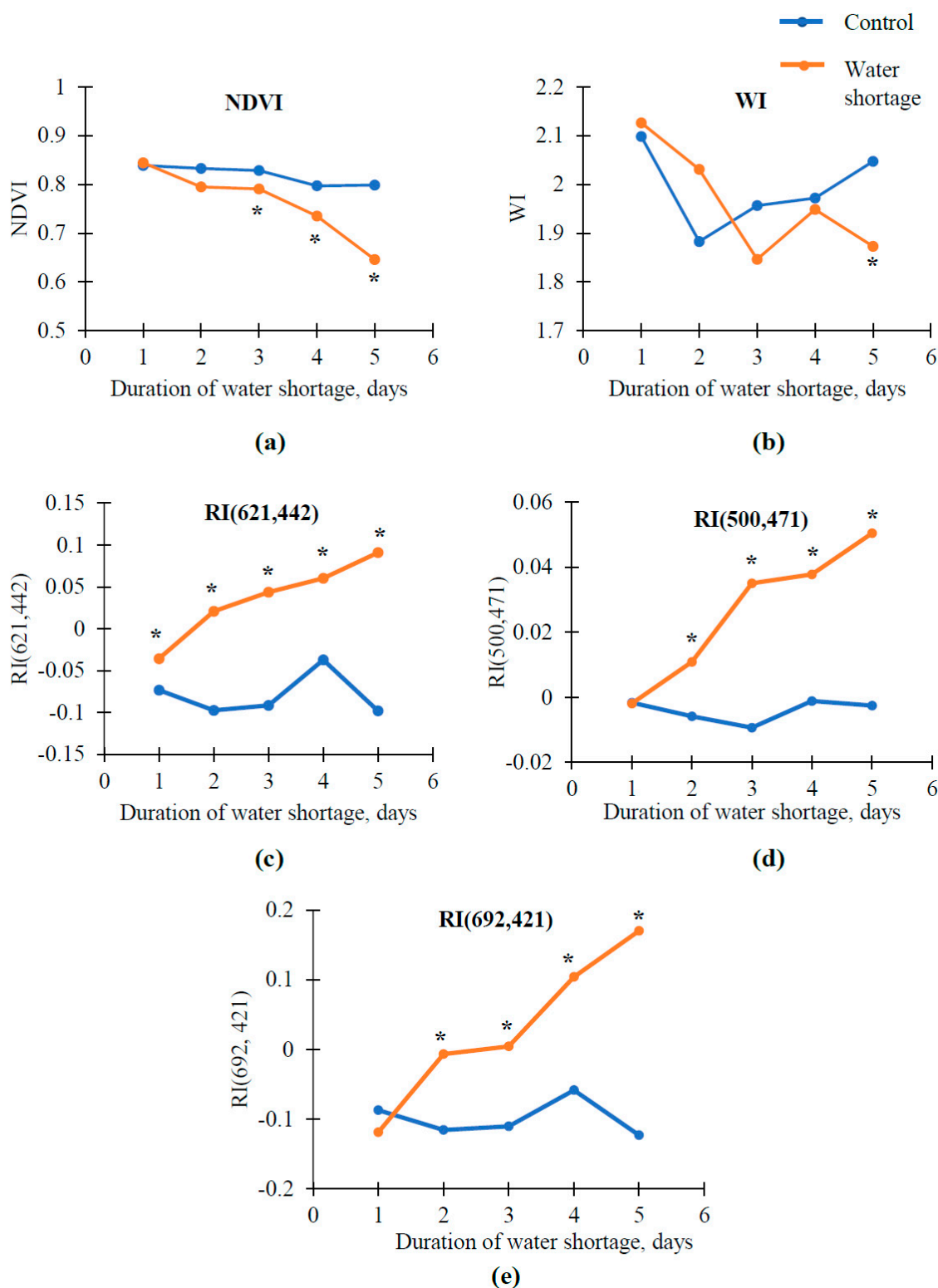


Figure 5. Dependence of (a) the normalized difference vegetation index (NDVI), (b) the water index (WI), (c) the difference reflectance index RI(621,442) was calculated based on $R_1 = 621$ nm and $R_2 = 442$ nm, (d) the difference reflectance index RI(500,471) was calculated based on $R_1 = 500$ nm and $R_2 = 471$ nm, and (e) the difference reflectance index RI(692,421) was calculated based on $R_1 = 692$ nm and $R_2 = 421$ nm for pea seedlings over duration of water shortage. Experimental plants were not irrigated; controls were irrigated every two days. Medians are shown in the figure. * Value significantly differed from control ($p < 0.05$, Mann-Whitney U test).

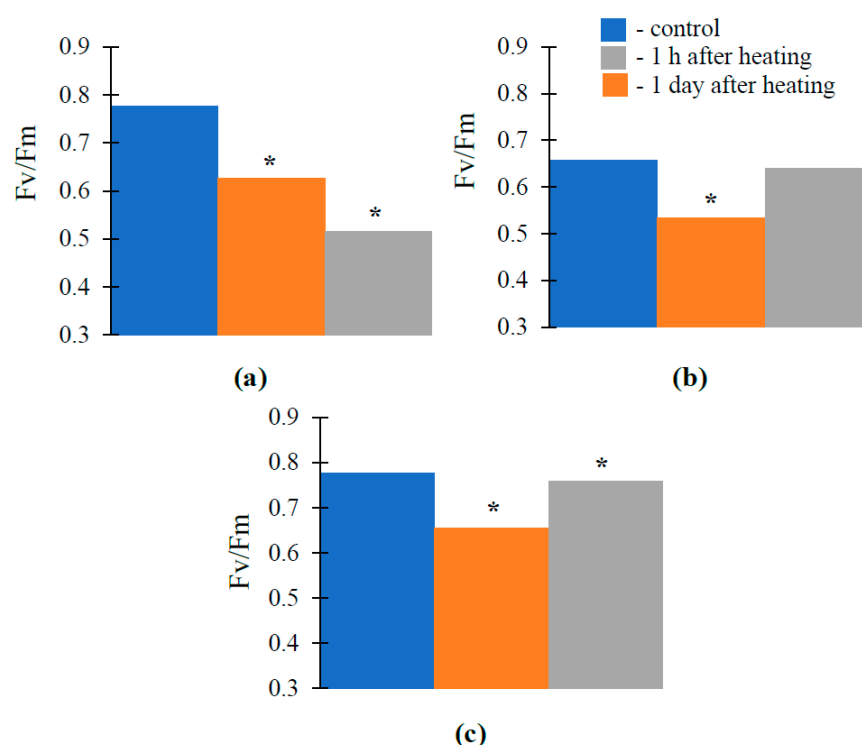


Figure 6. Maximal quantum yield of photosystem II (F_v/F_m) in control and in 1 h and one day after heating of whole plant for (a) pea, (b) wheat, and (c) pumpkin. Seedlings were heated in a TV-20-PZ-K thermostat for 30 min at 46.5 °C for pea and pumpkin and 44 °C for wheat. Medians are shown in the figure. * Value significantly differed from control ($p < 0.05$, Mann–Whitney U test).

Figure 8 shows that heatmaps of significances and directions of heating-induced changes in ΔRIs (the light-induced change in RIs). Several large spectral regions with significant differences between control and experimental seedlings (with increased and with decreased RIs) and several small regions were observed in pea, wheat, and pumpkin leaves in 1 h after heating. Some spectral ranges were specific for different investigated species. For example, a large spectral region with decreased ΔRIs (R_1 was about 525–575 nm, R_2 was about 460–540 nm) was observed in wheat seedlings in 1 h after the short-term heating but it was absent in pea and pumpkin seedlings. In contrast, some spectral ranges with significant changes in ΔRIs were observed in all investigated plants. For example, a large spectral region with decreased ΔRIs (R_1 was about 570–610 nm, R_2 was about 510–570 nm) was observed in all pea, wheat, and pumpkin seedlings in 1 h after the short-term heating.

The large areas of the spectral regions with changed ΔRIs were observed in one day after the short-term heating in pea seedlings. Some spectral regions were like the regions in 1 h after the heating; for example, the spectral region with decreased ΔRIs (R_1 was about 570–610 nm, R_2 was about 510–570 nm) or spectral region with increased ΔRIs (R_1 was about 675–700 nm, R_2 was about 400–650 nm). Only small spectral areas with significant changes in ΔRIs were observed in one day after the short-term heating in pumpkin seedlings. Finally, only separate pixels in the heatmap showed significant changes in ΔRIs in one day after the short-term heating in wheat seedlings. The results seemed to be similar to different recoveries of photosynthetic damages in different investigated species (the F_v/F_m recovery absence in pea seedlings and the partial recovery in wheat and pumpkin seedlings, Figure 6).

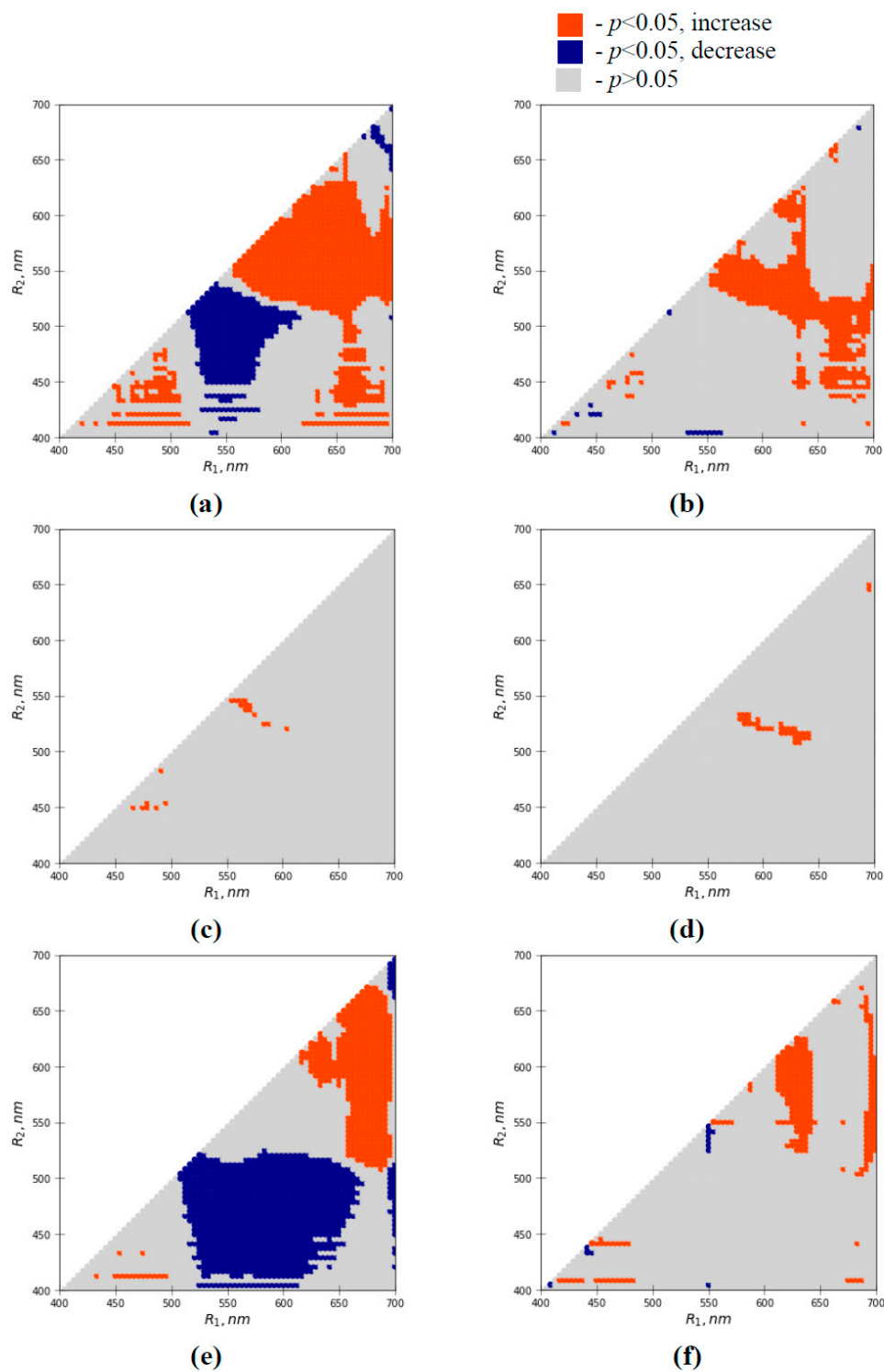


Figure 7. Heatmaps of significances and directions of heating-induced changes in absolute values of RIs in pea leaves in (a) 1 h and (b) one day after the heating, wheat leaves in (c) 1 h and (d) one day after the heating, and pumpkin leaves in (e) 1 h and (f) one day after the heating. RIs were calculated based on the equation $RI = \frac{I(R_1) - I(R_2)}{I(R_1) + I(R_2)}$, where $I(R_1)$ and $I(R_2)$ are intensities of reflected light at different narrow spectral bands (averaged for 3 nm). The Mann–Whitney U test was used for p calculations.

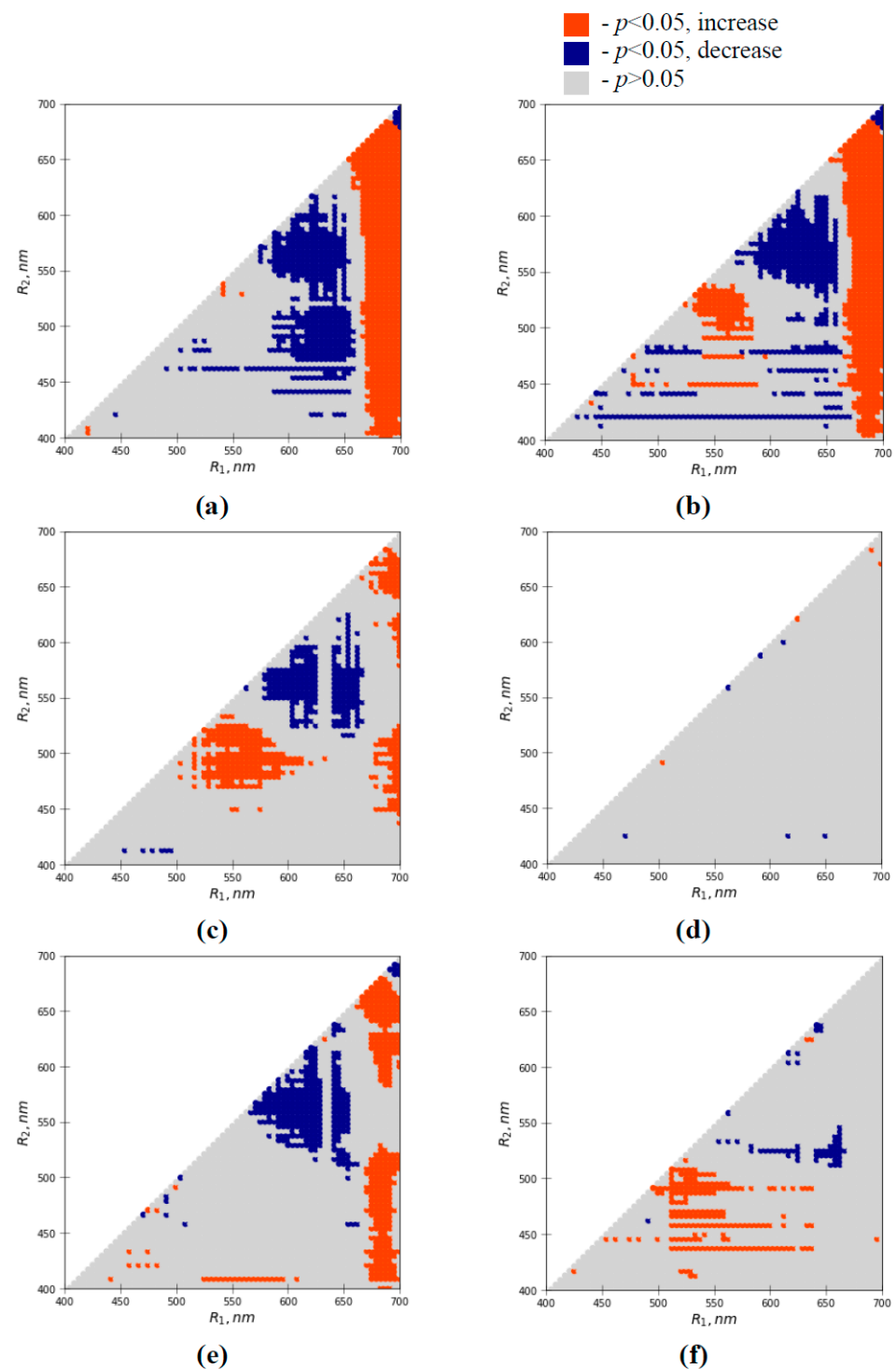


Figure 8. Heatmaps of significances and directions of heating-induced changes in ΔRIs in pea leaves in (a) 1 h and (b) one day after the heating, wheat leaves in (c) 1 h and (d) one day after the heating, and pumpkin leaves in (e) 1 h and (f) one day after the heating. RIs were calculated based on the equation $RI = \frac{I(R_1) - I(R_2)}{I(R_1) + I(R_2)}$, where $I(R_1)$ and $I(R_2)$ are intensities of reflected light at different narrow spectral bands (averaged for 3 nm). ΔRI (the light-induced change in RI) was calculated as $RI_2 - RI_1$. RI_1 was calculated based on $I(R_1)$ and $I(R_2)$ measured immediately after turning on the halogen lamp (first time point), and RI_2 based on $I(R_1)$ and $I(R_2)$ measured 7 min after turning on lamp (second time point). The Mann–Whitney U test was used for p calculations.

3.5. Analysis of Efficiencies of the Water Shortage-Sensitive Reflectance Indices for Revealing Heating-Induced Changes

Finally, we analyzed the question: Could the revealed RIs, which were sensitive to water shortage-induced changes (see Table 2), be significantly changed after the short-term heating? Only pea seedlings were investigated to increase accuracy of comparison between water shortage- and heating-induced changes in absolute values of RIs.

The two-dimensional data arrays, which included significances and directions of heating-induced changes for each RI as function of R_1 and R_2 , were directly analyzed. It was shown that 31 RIs from Table 2 were significantly increased in 1 h after the short-term heating and 2 RI was significantly increased in one day after that (Table 3). NDVI was significantly decreased in 1 h after the short-term heating; however, the significant change was absent in one day after the heating. Significant changes in WI were absent.

Table 3. Changes in absolute values of NDVI, WI, and the water shortage sensitive RIs (from Table 2) after the short-term heating.

Index	1 h	1 Day	Index	1 h	1 Day
NDVI	Decrease	-	RI(658; 421)	Increase	-
WI	-	-	RI(658; 442)	Increase	-
RI(487; 421)	Increase	-	RI(662; 421)	Increase	-
RI(491; 421)	Increase	-	RI(662; 442)	Increase	-
RI(496; 421)	Increase	-	RI(667; 421)	Increase	-
RI(496; 479)	Increase	-	RI(667; 442)	Increase	-
RI(500; 421)	Increase	-	RI(671; 421)	Increase	-
RI(500; 450)	Increase	-	RI(671; 433)	Increase	-
RI(504; 421)	Increase	-	RI(675; 421)	Increase	-
RI(504; 450)	Increase	-	RI(679; 421)	Increase	-
RI(508; 421)	Increase	-	RI(683; 421)	Increase	-
RI(613; 604)	Increase	Increase	RI(687; 421)	Increase	-
RI(633; 421)	Increase	-	RI(687; 433)	Increase	-
RI(633; 442)	Increase	-	RI(692; 421)	Increase	-
RI(637; 421)	Increase	-	RI(692; 442)	Increase	-
RI(654; 421)	Increase	-	RI(696; 421)	Increase	-
RI(654; 442)	Increase	-	RI(487; 458)	-	Increase

The RIs from Table 2, which were not significantly changed after the short-term heating, were not shown.

The results showed that there were RIs which were sensitive to both the water shortage and heating; however, the indices were mainly sensitive to plant changes, which were observed immediately after action of the increased temperature (in 1 h after the heating). Long-term changes in plants (changes, which were observed in one day after the heating) did not influence absolute values of 44 from 46 RIs, which were sensitive to the soil drought (see Tables 2 and 3).

4. Discussion

Soil drought, which is often accompanied by increased temperatures [11], is a key adverse factor for agricultural plants [5,8]. Early revelation of the water shortage action is a prospective way of the photosynthetic damage decrease and crop protection; the revelation can be based on the remote sensing of water shortage- and, maybe, heating-induced changes in plants [15–20]. Measurements of spectra of reflected light, which can be strongly related to content of pigments [18,40–46], photosynthetic processes [32–35], transpiration and water exchange [36–39], etc., can be effective tools for remote sensing of plant physiological processes [18,21,22,32] including the induction of stress changes [23,47,57–59].

There are numerous reflectance indices (e.g., NDVI, PRI, WI, NDWI, and NIR_V [33–36,39,42,48,74–79]) which are calculated on the basis of narrow spectral bands of reflected light and used for plant remote sensing. Using RIs for analysis of reflected light spectra has the number of preferences including the possibility to measure based on both multi- and hyperspectral cameras, simple algorithms for calculating RIs, the use of relative

units for RIs and minimization of errors related to light intensity, and the possibility to reveal specific physiological processes or specific physiological parameters related to specific wavelengths. The reflectance indices can be used for remote sensing of water shortage- and heating-induced changes in plants (e.g., NDVI, WI, NDWI, or PRI [54,76,77,81–83,92]).

However, current RIs are calculated on the basis of analysis of only small amounts of potential combinations of spectral bands; at that, even small shifts of the used wavelengths can modify the sensitivities of RIs to physiological processes (e.g., see [59]). As a result, the next step in development of methods of using RIs is their complex analysis, which includes estimation of efficiencies of all possible RIs, which are calculated based on all combinations of wavelengths of reflected light in the measured spectrum [51,85–89]. Construction of two-dimensional heatmaps, which show the efficiency of each possible RI (e.g., correlation coefficients between the RI and physiological parameters in correlograms [51,85–89]) as function of two wavelengths used for the calculation of this RI, is actively used for the complex analysis. In the current work, we analyze the similar heatmaps; however, significances and directions of water shortage- and heating-induced changes in RIs are estimated in our complex analysis. There are several important points which were shown in the current work.

First, we show that the heatmaps showing significances and directions of stressor-induced changes in RIs and Δ RIs (400–700 nm wavelength range) can be used for the complex revealing RIs and Δ RIs, which are sensitive to the short-term water shortage and heating (see Figures 3, 4, 7 and 8). In the heatmaps there are both spectral regions and separate pixels with significantly increased or decreased RIs and Δ RIs. It shows that both correlograms [51,85–89] and heatmaps of significances and directions of changes (our results) can be used for the analysis of efficiencies of reflectance indices as markers of stressor actions.

Second, the analysis of influencing the emulated water shortage on pea seedlings shows that water shortage-induced changes in absolute values of RIs are more expressive than the changes in Δ RIs (the light-induced change in RIs): the changes in RIs are initiated earlier (Figures 3 and 4) and spectral regions with these changes are larger (Table 1). There are both “specific” (significant changes in RIs are only observed at specific days after the water shortage initiation) and “universal” (significant changes in RIs are observed for several days of the water shortage action) spectral regions with drought-sensitive RIs in the heatmaps (Figure 3).

Further analysis shows that there are five RIs increased for 1–5 days of water shortage and other 41 RIs increased for 2–5 days of the shortage (Table 2). These RIs are more sensitive to water shortage than NDVI (increased for 3–5 days of water shortage) and WI (increased in 5th day), which are widely used for the remote sensing of drought-induced changes in plants [54,76,81–83]; the most of the RIs are strongly correlated to Fv/Fm and the relative water content in leaves. All 46 RIs are based on wavelengths related to absorption spectra for carotenoids and chlorophyll a and b [95]. It is additionally shown that at least some revealed RIs (e.g. RI(621,442), RI(500,471), and RI(692,421)) are more stable under control conditions than NDVI and WI (Figure 5). It is an important property because age-dependent dynamics of absolute value of reflectance index can strongly limit the RI using (e.g., changes in absolute value of PRI under control conditions can limit the index using for estimation of water shortage action on plants [92,96]). Considering absorption spectra for carotenoids and chlorophyll a and b [95], it can be additionally speculated that RI(621,442) is mainly related to the contents of carotenoids and chlorophyll a, RI(500,471) is mainly related to the contents of carotenoids and chlorophyll b, and RI(692,421) is probably related to the contents of chlorophyll a and b. Finally, 32 from these 46 RIs are also sensitive to short-term heating (Table 3), which is important considering the relations between drought and increased temperature [11].

Third, the analysis of influencing short-term heating on pea, wheat, and pumpkin seedlings shows that the heating influences absolute values of RIs in pea and pumpkin seedlings in a similar manner; in contrast, there are only minimal changes in RIs in wheat

seedlings (Figure 7). However, the analysis of ΔRIs (the light-induced change in RIs) shows that there are many spectral regions with significant changes in ΔRIs , which are similar in pea, wheat, and pumpkin seedlings at 1 h after the short-term heating (Figure 8). In one day after heating, the regions are minimal in wheat and pumpkin seedlings, but they remain in pea seedlings. Both results are in a good accordance with photosynthetic damage because Fv/Fm is significantly decreased 1 h after the short-term heating in pea, wheat, and pumpkin seedlings; in contrast, Fv/Fm partially recovers in wheat and pumpkin seedlings and is decreased in pea seedlings in one day after the heating.

It can be supposed that the differences in efficiency of RIs and ΔRIs can be related to the sensitivity of absolute values of the indices and their light-induced changes to different groups of processes. Changes in absolute values in RIs are probable to be mainly related to changes in content and composition of photosynthetic pigments [24,58], which can be affected by water shortage [97,98]. In contrast, ΔRIs are light-induced changes in RIs for 7 min of illumination. This means that ΔRIs should be related to light-induced physiological changes in this time interval. It is known that there are numerous photosynthetic changes, which are formed in this time interval (activation of electron transport chain [99], the formation of different components of non-photochemical quenching [100,101], changes in the electrochemical gradient of H^+ [100,102], etc.), and influence plant reflectance (e.g., [35,42,80]). Damaging the processes probably results in plant heating [92]; this damage can explain changes in ΔRIs in our experiments.

Thus, our results show that the complex analysis of efficiencies of RIs (and ΔRIs), which is based on the calculation of all reflectance indices (and their light-induced changes) in the measured spectral range of reflected light, on following the estimation of significances and directions of differences between RIs (and ΔRIs) in control and experimental plants, and on the construction of heatmaps of these significances and directions, which can be used for revealing new reflectance indices, and that are sensitive to stressors (by example of the 400–700 nm spectral range and the water shortage and heating).

It should be noted that our results are shown in laboratory experiments. It means that efficiencies of the specific RIs , which were sensitive to short-term water shortage in our work, require additional verification in field conditions in future. Potentially, efficiencies of revealed reflectance indices can be modified by complicated geometry of canopy in comparison to fixed leaf, fluctuations in environmental conditions (e.g., changes in light intensity or wind gusts), spatial heterogeneity in the investigated field (e.g., different plant growth density), etc. Additionally, it cannot be excluded that RIs , which are sensitive to early plant physiological changes under water shortage, will not be sensitive to physiological changes under long-term drought. As a result, further verification of the revealed specific indices in all noted cases is important problem of future investigations.

In contrast, it can be expected that the general proposed approach based on complex analysis of significance of changes in RIs and ΔRIs can be used for both leaf and canopy levels, different species, various stressors, different spatial and temporal scaled, etc. This means that the approach seems to be perspective for development of methods of remote sensing of action of stressors on agricultural plants in fields by multi- and hyper-spectral imaging that will increase food security and support a sustainable agriculture.

5. Conclusions

In the current work, we performed complex analysis of the efficiency of using difference reflectance indices for early revealing the influences of the short-term water shortage and heating on plant seedlings. In laboratory experiments, it was shown that calculation of all possible RIs and ΔRIs based on 400–700 nm spectral range and construction of heatmaps of significances of differences between control and experimental seedlings could be used for revealing indices, which were sensitive to plant changes induced by water shortage and heating. Using this approach, we showed that there were a number of RIs that were more sensitive to action of water shortage than NDVI and WI; some of the indices were also sensitive to heating action. It was additionally shown that absolute values of reflectance

indices were more sensitive to the action of water shortage. In contrast, light-induced changes in the indices were more sensitive to the action of heating.

New specific reflectance indices, which are sensitive to stressors in our work, can be potentially used for early revealing action of water shortage on plants; i.e., they can contribute to development of methods of plant remote sensing. However, a check of their efficiency in changeable environmental conditions, in different spatial and temporal scales, in different plant species, and under action of different stressors is an important future task because it cannot be excluded that efficiencies of the RIs may be strongly modified in these cases.

In contrast, it is very probable that the general proposed approach based on complex analysis of significance of changes in RIs and Δ RIs can be used for revealing reflectance indices, which will be effective tool for plant remote sensing at all noted cases. Therefore, another important task of future investigations is further analysis of efficiency of this approach for different experimental and field conditions.

Author Contributions: Conceptualization: E.S. and V.S.; methodology: E.S., L.Y., E.G., A.R., D.K., and V.S.; software: E.S.; formal analysis: E.S.; investigation: L.Y., E.G., A.R., and D.K.; writing—original draft: E.S.; writing—review and editing: V.S.; supervision: V.S.; project administration: E.S.; funding acquisition: E.S. and V.S. All authors have read and agreed to the published version of the manuscript.

Funding: The complex analysis of reflectance and photosynthetic changes under water shortage in pea seedlings was funded by the Russian Foundation for Basic Research, project number 20-016-00234 A. The complex analysis of reflectance and photosynthetic changes after heating in wheat seedlings was funded by the Russian Foundation for Basic Research, project number 20-316-80030 mol_ev_a. The complex analysis of reflectance and photosynthetic changes after heating in pea and pumpkin seedlings and revealing new reflectance indices were funded by the Russian Science Foundation, project number 17-76-20032.

Data Availability Statement: The data presented in this study are available on request from the corresponding author.

Conflicts of Interest: The authors declare no conflict of interest. The funders had no role in the design of the study; in the collection, analyses, or interpretation of data; in the writing of the manuscript, or in the decision to publish the results.

References

1. Battisti, D.S.; Naylor, R.L. Historical warnings of future food insecurity with unprecedented seasonal heat. *Science* **2009**, *323*, 240–244. [[CrossRef](#)]
2. Gornall, J.; Betts, R.; Burke, E.; Clark, R.; Camp, J.; Willett, K.; Wiltshire, A. Implications of climate change for agricultural productivity in the early twenty-first century. *Philos. Trans. R. Soc. B Biol. Sci.* **2010**, *365*, 2973–2989. [[CrossRef](#)]
3. Matsubara, S. Growing plants in fluctuating environments: Why bother? *J. Exp. Bot.* **2018**, *69*, 4651–4654. [[CrossRef](#)] [[PubMed](#)]
4. Zeppel, M.J.B.; Wilks, J.V.; Lewis, J.D. Impacts of extreme precipitation and seasonal changes in precipitation on plants. *Biogeosciences* **2014**, *11*, 3083–3093. [[CrossRef](#)]
5. Fahad, S.; Bajwa, A.A.; Nazir, U.; Anjum, S.A.; Farooq, A.; Zohaib, A.; Sadia, S.; Nasim, W.; Adkins, S.; Saud, S.; et al. Crop production under drought and heat stress: Plant responses and management options. *Front. Plant Sci.* **2017**, *8*, 1147. [[CrossRef](#)]
6. Quiles, M.J.; López, N.I. Photoinhibition of photosystems I and II induced by exposure to high light intensity during oat plant growth. Effects on the chloroplast NADH dehydrogenase complex. *Plant Sci.* **2004**, *166*, 815–823. [[CrossRef](#)]
7. Allakhverdiev, S.I.; Kreslavski, V.D.; Klimov, V.V.; Los, D.A.; Carpentier, R.; Mohanty, P. Heat stress: An overview of molecular responses in photosynthesis. *Photosynth. Res.* **2008**, *98*, 541–550. [[CrossRef](#)] [[PubMed](#)]
8. Gupta, A.; Rico-Medina, A.; Caño-Delgado, A.I. The physiology of plant responses to drought. *Science* **2020**, *368*, 266–269. [[CrossRef](#)]
9. Chaves, M.M.; Flexas, J.; Pinheiro, C. Photosynthesis under drought and salt stress: Regulation mechanisms from whole plant to cell. *Ann. Bot.* **2008**, *103*, 551–560. [[CrossRef](#)]
10. Zivcak, M.; Brestic, M.; Balatova, Z.; Drevenakova, P.; Olsovska, K.; Kalaji, H.M.; Yang, X.; Allakhverdiev, S.I. Photosynthetic electron transport and specific photoprotective responses in wheat leaves under drought stress. *Photosynth. Res.* **2013**, *117*, 529–546. [[CrossRef](#)]

11. Zandalinas, S.I.; Mittler, R.; Balfagón, D.; Arbona, V.; Gómez-Cadenas, A. Plant adaptations to the combination of drought and high temperatures. *Physiol. Plant.* **2018**, *162*, 2–12. [\[CrossRef\]](#)
12. Fromm, J.; Fei, H. Electrical signaling and gas exchange in maize plants of drying soil. *Plant Sci.* **1998**, *132*, 203–213. [\[CrossRef\]](#)
13. Du, C.; Chai, L.; Wang, Z.; Fan, H. Response of proteome and morphological structure to short-term drought and subsequent recovery in *Cucumis sativus* leaves. *Physiol. Plant.* **2019**, *167*, 676–689. [\[CrossRef\]](#) [\[PubMed\]](#)
14. Altuntaş, C.; Demiralay, M.; Sezgin Muslu, A.; Terzi, R. Proline-stimulated signaling primarily targets the chlorophyll degradation pathway and photosynthesis associated processes to cope with short-term water deficit in maize. *Photosynth. Res.* **2020**, *144*, 35–48. [\[CrossRef\]](#) [\[PubMed\]](#)
15. Pinter, P.J.J.; Hatfield, J.L.; Schepers, J.S.; Barnes, E.M.; Moran, M.S.; Daughtry, C.S.T.; Upchurch, D.R. Remote Sensing for Crop Management. *Photogramm. Eng. Remote Sens.* **2003**, *69*, 647–664. [\[CrossRef\]](#)
16. Yang, C. Remote Sensing and Precision Agriculture Technologies for Crop Disease Detection and Management with a Practical Application Example. *Engineering* **2020**, *6*, 528–532. [\[CrossRef\]](#)
17. Zarco-Tejada, P.J.; Berjón, A.; Miller, J.R. Stress detection in crops with hyperspectral remote sensing and physical simulation models. In Proceedings of the 2004 Airborne Imaging Spectroscopy Workshop, Bruges, Belgium, 8 October 2004; pp. 1–5.
18. Behmann, J.; Steinrücken, J.; Plümer, L. Detection of early plant stress responses in hyperspectral images. *ISPRS J. Photogramm. Remot. Sens.* **2014**, *93*, 98–111. [\[CrossRef\]](#)
19. Gerhards, M.; Schlerf, M.; Mallick, K.; Udelhoven, T. Challenges and future perspectives of multi-/hyperspectral thermal in-fared remote sensing for crop water-stress detection: A review. *Remote Sens.* **2019**, *11*, 1240. [\[CrossRef\]](#)
20. Mahlein, A.-K. Plant Disease Detection by Imaging Sensors—Parallels and Specific Demands for Precision Agriculture and Plant Phenotyping. *Plant Dis.* **2016**, *100*, 241–251. [\[CrossRef\]](#) [\[PubMed\]](#)
21. Mahlein, A.K.; Kuska, M.T.; Behmann, J.; Polder, G.; Walter, A. Hyperspectral sensors and imaging technologies in phytopathology: State of the art. *Annu. Rev. Phytopathol.* **2018**, *56*, 535–558. [\[CrossRef\]](#)
22. Prabhakar, M.; Prasad, Y.G.; Rao, M.N. Remote sensing of biotic stress in crop plants and its applications for pest management. In *Crop Stress and Its Management: Perspectives and Strategies*; Venkateswarlu, B., Shanker, A., Shanker, C., Maheswari, M., Eds.; Springer: Dordrecht, The Netherlands, 2012; pp. 517–545.
23. Gorbe, E.; Calatayud, A. Applications of chlorophyll fluorescence imaging technique in horticultural research: A review. *Sci. Hortic.* **2012**, *138*, 24–35. [\[CrossRef\]](#)
24. Porcar-Castell, A.; Tyystjärvi, E.; Atherton, J.; Van Der Tol, C.; Flexas, J.; Pfündel, E.E.; Moreno, J.; Frankenberg, C.; Berry, J.A. Linking chlorophyll a fluorescence to photosynthesis for remote sensing applications: Mechanisms and challenges. *J. Exp. Bot.* **2014**, *65*, 4065–4095. [\[CrossRef\]](#)
25. Zhang, C.; Atherton, J.; Peñuelas, J.; Filella, I.; Kolari, P.; Aalto, J.; Ruhanen, H.; Bäck, J.; Porcar-Castell, A. Do all chlorophyll fluorescence emission wavelengths capture the spring recovery of photosynthesis in boreal evergreen foliage? *Plant Cell Environ.* **2019**, *42*, 3264–3279. [\[CrossRef\]](#) [\[PubMed\]](#)
26. Sun, Y.; Fu, R.; Dickinson, R.; Joiner, J.; Frankenberg, C.; Gu, L.; Xia, Y.; Fernando, N. Drought onset mechanisms revealed by satellite solar-induced chlorophyll fluorescence: Insights from two contrasting extreme events. *J. Geophys. Res. Biogeosci.* **2015**, *120*, 2427–2440. [\[CrossRef\]](#)
27. Liu, L.; Yang, X.; Zhou, H.; Liu, S.; Zhou, L.; Li, X.; Yang, J.; Han, X.; Wu, J. Evaluating the utility of solar-induced chlorophyll fluorescence for drought monitoring by comparison with NDVI derived from wheat canopy. *Sci. Total Environ.* **2018**, *625*, 1208–1217. [\[CrossRef\]](#)
28. Wang, C.; Beringer, J.; Hutley, L.B.; Cleverly, J.; Li, J.; Liu, Q.; Sun, Y. Phenology Dynamics of Dryland Ecosystems Along the North Australian Transect Revealed by Satellite Solar-Induced Chlorophyll Fluorescence. *Geophys. Res. Lett.* **2019**, *46*, 5294–5302. [\[CrossRef\]](#)
29. Jones, H.G.; Stoll, M.; Santos, T.; de Sousa, C.; Chaves, M.M.; Grant, O.M. Use of infrared thermography for monitoring stomatal closure in the field: Application to grapevine. *J. Exp. Bot.* **2002**, *53*, 2249–2260. [\[CrossRef\]](#)
30. Jones, H.G.; Serraj, R.; Loveys, B.R.; Xiong, L.; Wheaton, A.; Price, A.H. Thermal infrared imaging of crop canopies for the remote diagnosis and quantification of plant responses to water stress in the field. *Funct. Plant Biol.* **2009**, *36*, 978–989. [\[CrossRef\]](#) [\[PubMed\]](#)
31. Lee, K.-J.; Lee, B.-W. Estimation of rice growth and nitrogen nutrition status using color digital camera image analysis. *Eur. J. Agron.* **2013**, *48*, 57–65. [\[CrossRef\]](#)
32. Gamon, J.A.; Huemmrich, K.F.; Wong, C.Y.S.; Ensminger, I.; Garrity, S.; Hollinger, D.Y.; Noormets, A.; Peñuelas, J. A remotely sensed pigment index reveals photosynthetic phenology in evergreen conifers. *Proc. Natl. Acad. Sci. USA* **2016**, *113*, 13087–13092. [\[CrossRef\]](#)
33. Peñuelas, J.; Garbulsky, M.F.; Filella, I. Photochemical reflectance index (PRI) and remote sensing of plant CO₂ uptake. *New Phytol.* **2011**, *191*, 596–599. [\[CrossRef\]](#) [\[PubMed\]](#)
34. Garbulsky, M.F.; Peñuelas, J.; Gamon, J.; Inoue, Y.; Filella, I. The photochemical reflectance index (PRI) and the remote sensing of leaf, canopy and ecosystem radiation use efficiencies. A review and meta-analysis. *Remote Sens. Environ.* **2011**, *115*, 281–297. [\[CrossRef\]](#)
35. Zhang, C.; Filella, I.; Garbulsky, M.F.; Peñuelas, J. Affecting factors and recent improvements of the photochemical reflectance index (PRI) for remotely sensing foliar, canopy and ecosystemic radiation-use efficiencies. *Remote Sens.* **2016**, *8*, 677. [\[CrossRef\]](#)

36. Peñuelas, J.; Filella, I.; Biel, C.; Serrano, L.; Savé, R. The reflectance at the 950–970 nm region as an indicator of plant water status. *Int. J. Remote Sens.* **1993**, *14*, 1887–1905. [\[CrossRef\]](#)
37. Sarlikioti, V.; Driever, S.; Marcelis, L. Photochemical reflectance index as a mean of monitoring early water stress. *Ann. Appl. Biol.* **2010**, *157*, 81–89. [\[CrossRef\]](#)
38. Zarco-Tejada, P.J.; González-Dugo, V.; Berni, J.A.J. Fluorescence, temperature and narrow-band indices acquired from a UAV platform for water stress detection using a micro-hyperspectral imager and a thermal camera. *Remote Sens. Environ.* **2012**, *117*, 322–337. [\[CrossRef\]](#)
39. Hmimina, G.; Dufrêne, E.; Soudani, K. Relationship between photochemical reflectance index and leaf ecophysiological and biochemical parameters under two different water statuses: Towards a rapid and efficient correction method using real-time measurements. *Plant Cell Environ.* **2014**, *37*, 473–487. [\[CrossRef\]](#)
40. Gerhards, M.; Schlerf, M.; Rascher, U.; Udelhoven, T.; Juszczak, R.; Alberti, G.; Miglietta, F.; Inoue, Y. Analysis of airborne optical and thermal imagery for detection of water stress symptoms. *Remote Sens.* **2018**, *10*, 1139. [\[CrossRef\]](#)
41. Jordan, C.F. Derivation of Leaf-Area Index from Quality of Light on the Forest Floor. *Ecology* **1969**, *50*, 663–666. [\[CrossRef\]](#)
42. Gamon, J.; Peñuelas, J.; Field, C. A narrow-waveband spectral index that tracks diurnal changes in photosynthetic efficiency. *Remote Sens. Environ.* **1992**, *41*, 35–44. [\[CrossRef\]](#)
43. Peñuelas, J.; Baret, F.; Filella, I. Semiempirical indices to assess carotenoids/chlorophyll a ratio from leaf spectral reflectance. *Photosynthetica* **1995**, *31*, 221–230.
44. Gamon, J.A.; Surfus, J.S. Assessing leaf pigment content and activity with a reflectometer. *New Phytol.* **1999**, *143*, 105–117. [\[CrossRef\]](#)
45. Gitelson, A.A.; Zur, Y.; Chivkunova, O.B.; Merzlyak, M.N. Assessing Carotenoid Content in Plant Leaves with Reflectance Spectroscopy. *Photochem. Photobiol.* **2007**, *75*, 272–281. [\[CrossRef\]](#)
46. Gitelson, A.A.; Chivkunova, O.B.; Merzlyak, M.N. Nondestructive estimation of anthocyanins and chlorophylls in anthocyanic leaves. *Am. J. Bot.* **2009**, *96*, 1861–1868. [\[CrossRef\]](#)
47. Peñuelas, J.; Gamon, J.; Fredeen, A.; Merino, J.; Field, C. Reflectance indices associated with physiological changes in nitrogen- and water-limited sunflower leaves. *Remote Sens. Environ.* **1994**, *48*, 135–146. [\[CrossRef\]](#)
48. Gamon, J.A.; Serrano, L.; Surfus, J.S. The photochemical reflectance index: An optical indicator of photosynthetic radiation use efficiency across species, functional types, and nutrient levels. *Oecologia* **1997**, *112*, 492–501. [\[CrossRef\]](#) [\[PubMed\]](#)
49. Shrestha, S.; Brueck, H.; Asch, F. Chlorophyll index, photochemical reflectance index and chlorophyll fluorescence measurements of rice leaves supplied with different N levels. *J. Photochem. Photobiol. B Biol.* **2012**, *113*, 7–13. [\[CrossRef\]](#) [\[PubMed\]](#)
50. Peñuelas, J.; Marino, G.; Llusia, J.; Morfopoulos, C.; Farré-Armengol, G.; Filella, I. Photochemical reflectance index as an indirect estimator of foliar isoprenoid emissions at the ecosystem level. *Nat. Commun.* **2013**, *4*, 2604. [\[CrossRef\]](#)
51. Balzarolo, M.; Peñuelas, J.; Filella, I.; Portillo-Estrada, M.; Ceulemans, R. Assessing ecosystem isoprene emissions by hyperspectral remote sensing. *Remote Sens.* **2018**, *10*, 1086. [\[CrossRef\]](#)
52. Sukhov, V.; Sukhova, E.; Gromova, E.; Surova, L.; Nerush, V.; Vodeneev, V. The electrical signal-induced systemic photosynthetic response is accompanied by changes in the photochemical reflectance index in pea. *Funct. Plant Biol.* **2019**, *46*, 328–338. [\[CrossRef\]](#) [\[PubMed\]](#)
53. Sukhova, E.; Yudina, L.; Akinchits, E.; Vodeneev, V.; Sukhov, V. Influence of electrical signals on pea leaf reflectance in the 400–800-nm range. *Plant Signal. Behav.* **2019**, *14*, 1610301. [\[CrossRef\]](#)
54. Sukhova, E.; Yudina, L.; Gromova, E.; Nerush, V.; Vodeneev, V.; Sukhov, V. Burning-induced electrical signals influence broadband reflectance indices and water index in pea leaves. *Plant Signal. Behav.* **2020**, *15*, 1737786. [\[CrossRef\]](#) [\[PubMed\]](#)
55. Gutiérrez, M.; Norton, R.; Thorp, K.R.; Wang, G. Association of Spectral Reflectance Indices with Plant Growth and Lint Yield in Upland Cotton. *Crop. Sci.* **2012**, *52*, 849–857. [\[CrossRef\]](#)
56. Brandão, Z.N.; Sofiatti, V.; Bezerra, J.R.C.; Ferreira, G.B.; Medeiros, J.C. Spectral reflectance for growth and yield assessment of irrigated cotton. *AJCS* **2015**, *9*, 75–84.
57. Evain, S.; Flexas, J.; Moya, I. A new instrument for passive remote sensing: 2. Measurement of leaf and canopy reflectance changes at 531 nm and their relationship with photosynthesis and chlorophyll fluorescence. *Remote Sens. Environ.* **2004**, *91*, 175–185. [\[CrossRef\]](#)
58. Filella, I.; Porcar-Castell, A.; Munne-Bosch, S.; Bäck, J.; Garbulsky, M.F.; Peñuelas, J. PRI assessment of long-term changes in carotenoids/chlorophyll ratio and short-term changes in de-epoxidation state of the xanthophyll cycle. *Int. J. Remote Sens.* **2009**, *30*, 4443–4455. [\[CrossRef\]](#)
59. Sukhova, E.; Sukhov, V. Relation of Photochemical Reflectance Indices Based on Different Wavelengths to the Parameters of Light Reactions in Photosystems I and II in Pea Plants. *Remote Sens.* **2020**, *12*, 1312. [\[CrossRef\]](#)
60. Mahlein, A.K.; Steiner, U.; Dehne, H.W.; Oerke, E.C. Spectral signatures of sugar beet leaves for the detection and differentiation of diseases. *Precis. Agric.* **2010**, *11*, 413–431. [\[CrossRef\]](#)
61. Zhu, H.; Chu, B.; Zhang, C.; Liu, F.; Jiang, L.; He, Y. Hyperspectral Imaging for Presymptomatic Detection of Tobacco Disease with Successive Projections Algorithm and Machine-learning Classifiers. *Sci. Rep.* **2017**, *7*, 1–12. [\[CrossRef\]](#)
62. Fu, P.; Meacham-Hensold, K.; Guan, K.; Bernacchi, C.J. Hyperspectral Leaf Reflectance as Proxy for Photosynthetic Capacities: An Ensemble Approach Based on Multiple Machine Learning Algorithms. *Front. Plant Sci.* **2019**, *10*, 730. [\[CrossRef\]](#)

63. Gold, K.M.; Townsend, P.A.; Herrmann, I.; Gevens, A.J. Investigating potato late blight physiological differences across potato cultivars with spectroscopy and machine learning. *Plant Sci.* **2020**, *295*, 110316. [[CrossRef](#)] [[PubMed](#)]
64. Sonobe, R.; Hirono, Y.; Oi, A. Non-Destructive Detection of Tea Leaf Chlorophyll Content Using Hyperspectral Reflectance and Machine Learning Algorithms. *Plants* **2020**, *9*, 368. [[CrossRef](#)] [[PubMed](#)]
65. Singh, A.K.; Ganapathysubramanian, B.; Sarkar, S.; Singh, A. Deep learning for plant stress phenotyping: Trends and future perspectives. *Trends Plant Sci.* **2018**, *23*, 883–898. [[CrossRef](#)]
66. Paulus, S.; Mahlein, A.-K. Technical workflows for hyperspectral plant image assessment and processing on the greenhouse and laboratory scale. *GigaScience* **2020**, *9*, 90. [[CrossRef](#)]
67. Jacquemoud, S.; Baret, F. PROSPECT: A model of leaf optical properties spectra. *Remote Sens. Environ.* **1990**, *34*, 75–91. [[CrossRef](#)]
68. Zhang, Y.; Huang, J.; Wang, F.; Blackburn, G.A.; Zhang, H.K.; Wang, X.; Wei, C.; Zhang, K.; Wei, C. An extended PRO-SPECT: Advance in the leaf optical properties model separating total chlorophylls into chlorophyll a and b. *Sci. Rep.* **2017**, *7*, 6429. [[CrossRef](#)]
69. Jiang, J.; Comar, A.; Burger, P.; Bancal, P.; Weiss, M.; Baret, F. Estimation of leaf traits from reflectance measurements: Comparison between methods based on vegetation indices and several versions of the PROSPECT model. *Plant Methods* **2018**, *14*, 23. [[CrossRef](#)] [[PubMed](#)]
70. Ustin, S.L.; Jacquemoud, S.; Govaerts, Y. Simulation of photon transport in a three-dimensional leaf: Implications for photosynthesis. *Plant Cell Environ.* **2001**, *24*, 1095–1103. [[CrossRef](#)]
71. Hikosaka, K.; Kumagai, T.; Ito, A. Modeling canopy photosynthesis. In *Canopy Photosynthesis: From Basics to Applications. Advances in Photosynthesis and Respiration (Including Bioenergy and Related Processes)*; Hikosaka, K., Niinemets, Ü., Anten, N., Eds.; Springer: Dordrecht, The Netherlands, 2016; pp. 239–268.
72. Evers, J.B.; Vos, J.; Yin, X.; Romero, P.; Van Der Putten, P.E.L.; Struik, P.C. Simulation of wheat growth and development based on organ-level photosynthesis and assimilate allocation. *J. Exp. Bot.* **2010**, *61*, 2203–2216. [[CrossRef](#)]
73. Hao, D.; Wen, J.; Xiao, Q.; Wu, S.; Lin, X.; You, D.; Tang, Y. Modeling Anisotropic Reflectance Over Composite Sloping Terrain. *IEEE Trans. Geosci. Remote Sens.* **2018**, *56*, 3903–3923. [[CrossRef](#)]
74. Rouse, J.W., Jr.; Haas, R.H.; Schell, J.A.; Deering, D.W.; Harlan, J.C. *Monitoring the Vernal Advancement and Retrogradation (Green Wave Effect) of Natural Vegetation*; Type III Final Rep; The National Aeronautics and Space Administration (NASA)/Goddard Space Flight Center (GSFC): Greenbelt, MD, USA, 1974.
75. Eitel, J.U.H.; Long, D.S.; Gessler, P.E.; Hunt, E.R., Jr.; Brown, D.J. Sensitivity of ground-based remote sensing estimates of wheat chlorophyll content to variation in soil reflectance. *Soil Sci. Soc. Am. J.* **2009**, *73*, 1715–1723. [[CrossRef](#)]
76. Penuelas, J.P.J.; Pinol, J.; Ogaya, R.; Filella, I. Estimation of plant water concentration by the reflectance Water Index WI (R900/R970). *Int. J. Remote Sens.* **1997**, *18*, 2869–2875. [[CrossRef](#)]
77. Gao, B.-C. NDWI—A normalized difference water index for remote sensing of vegetation liquid water from space. *Remote Sens. Environ.* **1996**, *58*, 257–266. [[CrossRef](#)]
78. Sukhova, E.; Sukhov, V. Connection of the Photochemical Reflectance Index (PRI) with the Photosystem II Quantum Yield and Nonphotochemical Quenching Can Be Dependent on Variations of Photosynthetic Parameters among Investigated Plants: A Meta-Analysis. *Remote Sens.* **2018**, *10*, 771. [[CrossRef](#)]
79. Badgley, G.; Field, C.B.; Berry, J.A. Canopy near-infrared reflectance and terrestrial photosynthesis. *Sci. Adv.* **2017**, *3*, e1602244. [[CrossRef](#)]
80. Sukhova, E.M.; Yudina, L.M.; Vodeneev, V.A.; Sukhov, V.S. Analysis of Changes in Photochemical Reflectance Index (PRI) in Relation to the Acidification of the Lumen of the Chloroplasts of Pea and Geranium Leaves under a Short-Term Illumination. *Biochem. Suppl. Ser. A Membr. Cell Biol.* **2019**, *13*, 243–252. [[CrossRef](#)]
81. Ali, S.; Henchiri, M.; Yao, F.; Zhang, J. Analysis of vegetation dynamics, drought in relation with climate over South Asia from 1990 to 2011. *Environ. Sci. Pollut. Res.* **2019**, *26*, 11470–11481. [[CrossRef](#)]
82. Zhang, F.; Zhou, G. Estimation of vegetation water content using hyperspectral vegetation indices: A comparison of crop water indicators in response to water stress treatments for summer maize. *BMC Ecol.* **2019**, *19*, 18. [[CrossRef](#)]
83. Caturegli, L.; Matteoli, S.; Gaetani, M.; Grossi, N.; Magni, S.; Minelli, A.; Corsini, G.; Remorini, D.; Volterrani, M. Effects of water stress on spectral reflectance of bermudagrass. *Sci. Rep.* **2020**, *10*, 1–12. [[CrossRef](#)] [[PubMed](#)]
84. Wang, K.; Zhang, X.; Goatley, M.; Ervin, E. Heat Shock Proteins in Relation to Heat Stress Tolerance of Creeping Bentgrass at Different N Levels. *PLoS ONE* **2014**, *9*, e102914. [[CrossRef](#)]
85. Sytar, O.; Brücková, K.; Kovár, M.; Živčák, M.; Hemmerich, I.; Brestič, M. Nondestructive detection and biochemical quantification of buckwheat leaves using visible (VIS) and near-infrared (NIR) hyperspectral reflectance imaging. *J. Cent. Eur. Agric.* **2017**, *18*, 864–878. [[CrossRef](#)]
86. Kovar, M.; Brestic, M.; Sytar, O.; Barek, V.; Hauptvogel, P.; Zivcak, M. Evaluation of Hyperspectral Reflectance Parameters to Assess the Leaf Water Content in Soybean. *Water* **2019**, *11*, 443. [[CrossRef](#)]
87. El-Hendawy, S.; Al-Suhaibani, N.; Dewir, Y.H.; Elsayed, S.; Alotaibi, M.; Hassan, W.; Refay, Y.; Tahir, M.U. Ability of modified spectral reflectance indices for estimating growth and photosynthetic efficiency of wheat under saline field conditions. *Agronomy* **2019**, *9*, 35. [[CrossRef](#)]

88. El-Hendawy, S.E.; Alotaibi, M.; Al-Suhaibani, N.; Al-Gaadi, K.; Hassan, W.; Dewir, Y.H.; Emam, M.A.E.-G.; Elsayed, S.; Schmidhalter, U. Comparative Performance of Spectral Reflectance Indices and Multivariate Modeling for Assessing Agronomic Parameters in Advanced Spring Wheat Lines Under Two Contrasting Irrigation Regimes. *Front. Plant Sci.* **2019**, *10*, 1537. [[CrossRef](#)] [[PubMed](#)]
89. Sun, H.; Feng, M.; Xiao, L.; Yang, W.; Wang, C.; Jia, X.; Zhao, Y.; Zhao, C.; Muhammad, S.K.; Li, D. Assessment of plant water status in winter wheat (*Triticum aestivum* L.) based on canopy spectral indices. *PLoS ONE* **2019**, *14*, e0216890. [[CrossRef](#)]
90. Balegh, S.E.; Biddulph, O. The Photosynthetic Action Spectrum of the Bean Plant. *Plant Physiol.* **1970**, *46*, 1–5. [[CrossRef](#)]
91. Inada, K. Action spectra for photosynthesis in higher plants. *Plant Cell Physiol.* **1976**, *17*, 355–365. [[CrossRef](#)]
92. Yudina, L.; Sukhova, E.; Gromova, E.; Nerush, V.; Vodeneev, V.; Sukhov, V. A light-induced decrease in the photochemical reflectance index (PRI) can be used to estimate the energy-dependent component of non-photochemical quenching under heat stress and soil drought in pea, wheat, and pumpkin. *Photosynth. Res.* **2020**, *146*, 175–187. [[CrossRef](#)]
93. Sukhov, V.S.; Gromova, E.N.; Sukhova, E.M.; Surova, L.M.; Nerush, V.N.; Vodeneev, V.A. Analysis of Correlations between the Indexes of Light-Dependent Reactions of Photosynthesis and the Photochemical Reflectance Index (PRI) in Pea Leaves under Short-Term Illumination. *Biochem. Suppl. Ser. A Membr. Cell Biol.* **2019**, *13*, 67–77. [[CrossRef](#)]
94. Kalaji, H.M.; Schansker, G.; Ladle, R.J.; Goltsev, V.; Bosa, K.; Allakhverdiev, S.I.; Brestic, M.; Bussotti, F.; Calatayud, A.; Dąbrowski, P.; et al. Frequently asked questions about in vivo chlorophyll fluorescence: Practical issues. *Photosynth. Res.* **2014**, *122*, 121–158. [[CrossRef](#)]
95. Whitmarsh, J. The Photosynthetic Process. In *Concepts in Photobiology*; Singhal, G.S., Renger, G., Sopory, S.K., Irrgang, K.D., Eds.; Springer: Dordrecht, The Netherlands, 1999; pp. 11–51.
96. Sukhova, E.; Sukhov, V. Analysis of Light-Induced Changes in the Photochemical Reflectance Index (PRI) in Leaves of Pea, Wheat, and Pumpkin Using Pulses of Green-Yellow Measuring Light. *Remote Sens.* **2019**, *11*, 810. [[CrossRef](#)]
97. Sun, P.; Wahbi, S.; Tsonev, T.; Haworth, M.; Liu, S.; Centritto, M. On the Use of Leaf Spectral Indices to Assess Water Status and Photosynthetic Limitations in *Olea europaea* L. during Water-Stress and Recovery. *PLoS ONE* **2014**, *9*, e105165. [[CrossRef](#)] [[PubMed](#)]
98. Bayat, B.; Van Der Tol, C.; Verhoef, W. Remote Sensing of Grass Response to Drought Stress Using Spectroscopic Techniques and Canopy Reflectance Model Inversion. *Remote Sens.* **2016**, *8*, 557. [[CrossRef](#)]
99. Sukhova, E.; Khlopkov, A.; Vodeneev, V.; Sukhov, V. Simulation of a nonphotochemical quenching in plant leaf under different light intensities. *Biochim. Biophys. Acta Bioenerg.* **2020**, *1861*, 148138. [[CrossRef](#)] [[PubMed](#)]
100. Müller, P.; Li, X.-P.; Niyogi, K.K. Non-Photochemical Quenching. A Response to Excess Light Energy. *Plant Physiol.* **2001**, *125*, 1558–1566. [[CrossRef](#)] [[PubMed](#)]
101. Ruban, A.V. Nonphotochemical Chlorophyll Fluorescence Quenching: Mechanism and Effectiveness in Protecting Plants from Photodamage. *Plant Physiol.* **2016**, *170*, 1903–1916. [[CrossRef](#)] [[PubMed](#)]
102. Demmig-Adams, B. Carotenoids and photoprotection in plants: A role for the xanthophyll zeaxanthin. *Biochim. Biophys. Acta (BBA) Bioenerg.* **1990**, *1020*, 1–24. [[CrossRef](#)]